REC-ERC-74-12

HYDRAULIC MODEL STUDIES FOR THE PENSTOCKS FOR GRAND COULEE THIRD POWERPLANT

Engineering and Research Center
Bureau of Reclamation

August 1974

MS-230 (8-70)
Bureau of Reclamation

TECHNICAL REPORT STANDARD TITLE PAGE

1. REPORT NO.	2. GOVERNMENT ACCESSION NO.	3. RECIPIENT'S CATALOG NO.
REC-ERC-74-12		

4. TITLE AND SUBTITLE	5. REPORT DATE
Hydraulic Model Studies for the Penstocks for Grand Coulee Third Powerplant	August 1974
	6. PERFORMING ORGANIZATION CODE
7. AUTHOR(S):	8. PERFORMING ORGANIZATION REPORT NO.
T. J. Rhone	REC-ERC-74-12
9. PERFORMING ORGANIZATION NAME AND ADDRESS	10. WORK UNIT NO.
Engineering and Research Center Bureau of Reclamation Denver, Colorado 80225	11. CONTRACT OR GRANT NO.
	13. TYPE OF REPORT AND PERIOD COVERED
12. SPONSORING AGENCY NAME AND ADDRESS	14. SPONSORING AGENCY CODE

15. SUPPLEMENTARY NOTES

16. ABSTRACT

Hydraulic model investigations were performed on a 1:41.75 scale model to aid in the design of the penstock entrances and lower bends of the Third Powerplant at Grand Coulee Dam. The initial entrance with a 2:1 height-to-width ratio, entrance area equal to penstock area, and a small radius entrance curve indicated excessive head loss and poor pressure distribution along the flow surfaces. A longer compound radius entrance curve reduced the head loss and improved the pressure distribution along the flow surfaces. A more economical entrance with a 1-1/2:1 height-to-width ratio and the compound radius entrance curve showed excellent hydraulic characteristics and was selected for prototype installation. The proposed trashrack will add to the head loss but will not affect other flow conditions. A model with flared entrance curves on the left side and roof was also tested but showed no significant improvements in flow characteristics. A model with the entrance area equal to 9/10 the penstock area indicated excessive head loss and poor pressure conditions. Vortex observations indicated the possibility of air-entraining vortices with all entrances tested. More detailed vortex studies on another model will be reported separately. Three types of lower bends were investigated. None showed any particular hydraulic advantage.

17. KEY WORDS AND DOCUMENT ANALYSIS

a. DESCRIPTORS-- / bellmouths/ bends (hydraulic)/ *entrances (fluid flow)/ *head losses/ *hydraulic models/ intake structures/ *penstocks/ intake transitions/ trashracks/ turbulence/ *velocity distribution/ vortices/ prototypes/ model tests/ pressure distribution/ flow characteristics/ entrapped air

b. IDENTIFIERS-- / Grand Coulee Powerplant, WA

c. COSATI Field/Group 13M

18. DISTRIBUTION STATEMENT	19. SECURITY CLASS (THIS REPORT)	21. NO. OF PAGES
Available from the National Technical Information Service, Operations Division, Springfield, Virginia 22151.	UNCLASSIFIED	41
	20. SECURITY CLASS (THIS PAGE) UNCLASSIFIED	22. PRICE

REC-ERC-74-12

HYDRAULIC MODEL STUDIES FOR THE PENSTOCKS FOR GRAND COULEE THIRD POWERPLANT

by
T. J. Rhone

August 1974

Hydraulics Branch
Division of General Research
Engineering and Research Center
Bureau of Reclamation
Denver, Colorado

UNITED STATES DEPARTMENT OF THE INTERIOR * BUREAU OF RECLAMATION

ACKNOWLEDGMENT

This study was conducted with the cooperation of the Concrete Dams Section of the Hydraulic Structures Branch and the Hydraulic Machinery Section of the Mechanical Branch, Division of Design. The study was performed by the author under the supervision of W. E. Wagner, Head, Applied Hydraulics Section (now Chief, Hydraulics Branch), Division of Research.

CONTENTS

CONTENTS—Continued

LIST OF FIGURES

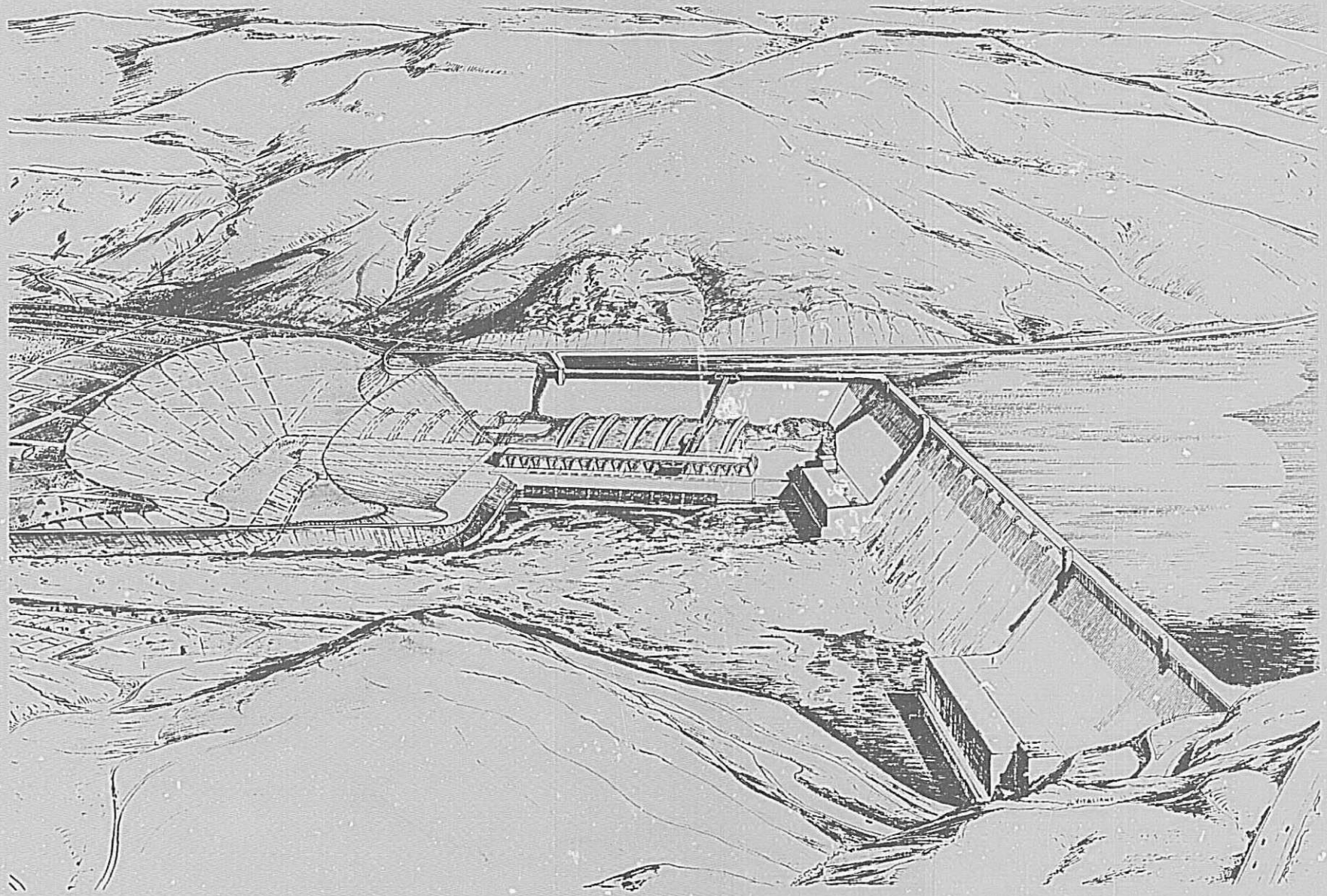

GRAND COULEE THIRD POWER PLANT

Figure 1

PURPOSE

The purpose of the study was to aid in developing the designs of the penstock entrance and lower bend for the Third Powerplant at Grand Coulee Dam.

RESULTS

1. The entrance curve of the initial penstock entrance was too abrupt as shown by the high head loss (0.19 h_v) and the pressure drop coefficients, Figure 6.

2. Replacing the abrupt entrance curve with a longer more gradual curve reduced the head loss coefficient to 0.14. The pressure distribution on the entrance boundaries was also improved, Figure 8.

3. To reduce the overall cost of the structure, the height-to-width ratio of the entrance was changed from 2:1 to 1-1/2:1. With the same gradual entrance curves used in the modified original entrance the head loss coefficient dropped to 0.13. Pressure distribution on the boundaries was about the same.

4. Vortex tendencies were about the same for both entrances and indicated that there might be vortex action within the anticipated operating limits.

5. The recommended entrance based on a smaller bellmouth, a 1-1/2:1 height-to-width ratio, and incorporating necessary structural considerations was constructed for the model, Figure 11. The head loss coefficient with this configuration was 0.08, Figure 12. Because of the flat surface at the start of the entrance curves, the pressure distribution on the boundaries was not as good as in the previous designs, Figure 13. Pressure fluctuation on the boundaries was also adversely affected by the geometry, particularly with asymmetrical approach flow, but was not considered unsatisfactory. Velocity distribution in the penstock was very good, Figure 14. There was some turbulent flow in the penstock with asymmetrical approach flow.

6. To try to alleviate some of the adverse flow conditions found with asymmetrical approach flow, an entrance with flared entrance curves on the left side and top was tested, Figure 15. The head loss and pressure drop coefficients, the pressure fluctuations, and the velocity distribution were slightly improved with the flared entrance. However, turbulence in the penstock was much worse. Because of the excessive turbulence and the larger size stoplogs required, a symmetrical entrance for prototype installation was used.

7. The proposed trashrack will add to the head loss, but should not cause significant difference in the pressure drop or velocity distribution in the entrance.

8. A smaller model with an entrance area to penstock area ratio of 0.9:1 was also tested. In all tests this entrance showed poorer hydraulic conditions.

9. Three types of lower bends were investigated. No particular comparative hydraulic advantages were noted.

APPLICATIONS

Although these tests were performed to aid in the development of the penstocks for the Grand Coulee Third Powerplant, the data have been presented in a dimensionless form that can be used in the design of other low velocity conduits or penstock entrances.

INTRODUCTION

Grand Coulee Dam is on the Columbia River about 90 miles (145 km) west of Spokane, Washington. The original dam was constructed during the period 1933 to 1942. The primary hydraulic features of the dam include a spillway, multiple outlet works, a powerplant on each abutment, and a pump-storage facility in the left abutment.

The Columbia River Treaty with Canada made possible additional storage capacity upstream from Grand Coulee Dam. Previously, water has been wasted over the spillway. Therefore, the Third Powerplant was conceived to utilize this flow and become a profitable addition to the Grand Coulee complex.

Based on current (1974) planning, the Third Powerplant, Figure 1, will have an ultimate capacity of more than 8,100 megawatts (MW) through 12 generating units. Six units are authorized. Three 600-MW units are now under construction and the other three authorized units will be increased in size to 700 MW.

Three hydraulic model studies were made during the development of the Third Powerplant design. The first study was to confirm the design of the forebay channel and tailrace for both 6- and 12-unit configurations. The results of this study have been reported in Report No. REC-ERC-73-2, "Hydraulic Model Studies for Grand Coulee Third Powerplant Forebay and Tailrace

Channels," by D. L. King. The second study was to aid in the development of the penstock design and is the subject of this report. The third study was to determine the vortex characteristics of the forebay channel and tailrace. The results of the vortex study is contained in a report by E. R. Zeigler entitled, "Hydraulic Model Vortex Tests–Grand Coulee Third Powerplant."

THE MODEL

The studies described herein were performed on a 1:41.74 scale model of the penstock and included the penstock entrance; transition between the entrance and penstock; and the penstock, including the two vertical bends, down to the scrollcase, Figure 2.

The 40-foot (12.18-meter) diameter penstock was represented by 11.5-inch (39.6-cm) diameter clear plastic pipe. The penstock entrance and the elbows were also constructed of clear plastic. Water was supplied to the model penstock entrance through a 12-foot (3.7-meter) square by 14-foot (4.3-meter) high tank to represent flow from the reservoir.

Discharge quantities were measured with Venturi meters in the permanent laboratory supply system. Pressures were measured by piezometers connected to open tube water manometers or pressure transducers. Velocity measurements in the penstock were made by pitot cylinders connected to water manometers. Turbulence determinations were obtained by placing a pressure transducer on the impact lead of the pitot cylinder and recording the instantaneous fluctuations on an oscillograph. Reservoir elevations and ambient pressures in the penstocks were obtained by piezometers connected to water manometers.

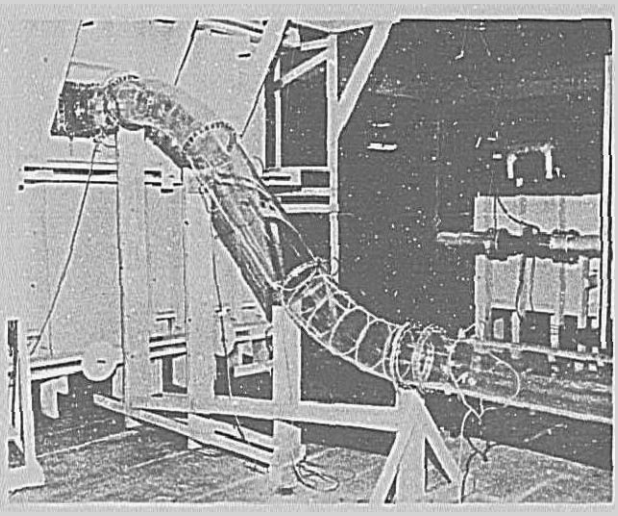

Figure 2. 1:41.74 scale model of penstock. Photo P1222-D-74685

The model was designed and all test results were analyzed on the basis of the Froude relationship. The limited vortex observations reported were also made with the penstock discharge (and flow velocity) based on the Froude relationship. Some authorities believe that vortex characteristics should be studied on an equal velocity basis, which would require that the model penstock flow velocity be the same as the prototype velocity, or for this study, 27.7 ft/sec (8.5 meters). This would have required a model discharge of almost 20 cfs (0.57 cu m/sec), which could not be attained in this test facility.

THE INVESTIGATION

In 1966, a Value Engineering Team was formed in the Engineering and Research Center in Denver to systematically analyze the procedures used to design a penstock entrance. The team concluded that the then current design practices could be modified to provide a substantial reduction in costs without sacrificing the basic functions or safety of the structure. Included in the recommended modifications were reductions in the size of the bellmouth entrance and gate and simplification of the entrance curves.

The modified design principles recommended by the team were used in the design of the penstock entrances for the Third Powerplant. Since this design was a departure from accepted practices, hydraulic model studies were used to aid in developing the entrance and to verify the design of the entrance, transition, and penstock down to the scrollcase.

Preliminary Entrance Studies

Initial entrance.—The initial entrance utilized a very small, simple radius, bellmouth entrance curve, a gate section with a height-to-width ratio of 2:1, a gate area-to-penstock area ratio of 1.00, and a constant area transition between the gate section and the penstock, Figure 3.

The head loss through the entrance and the pressure distribution on the entrance boundary surfaces were evaluated. The head loss was measured from the reservoir to a point midway between the end of the transition and the start of the curve (P.C.) of the upper penstock elbow, Figure 4. This measurement included the losses caused by the bellmouth entrance curve, the

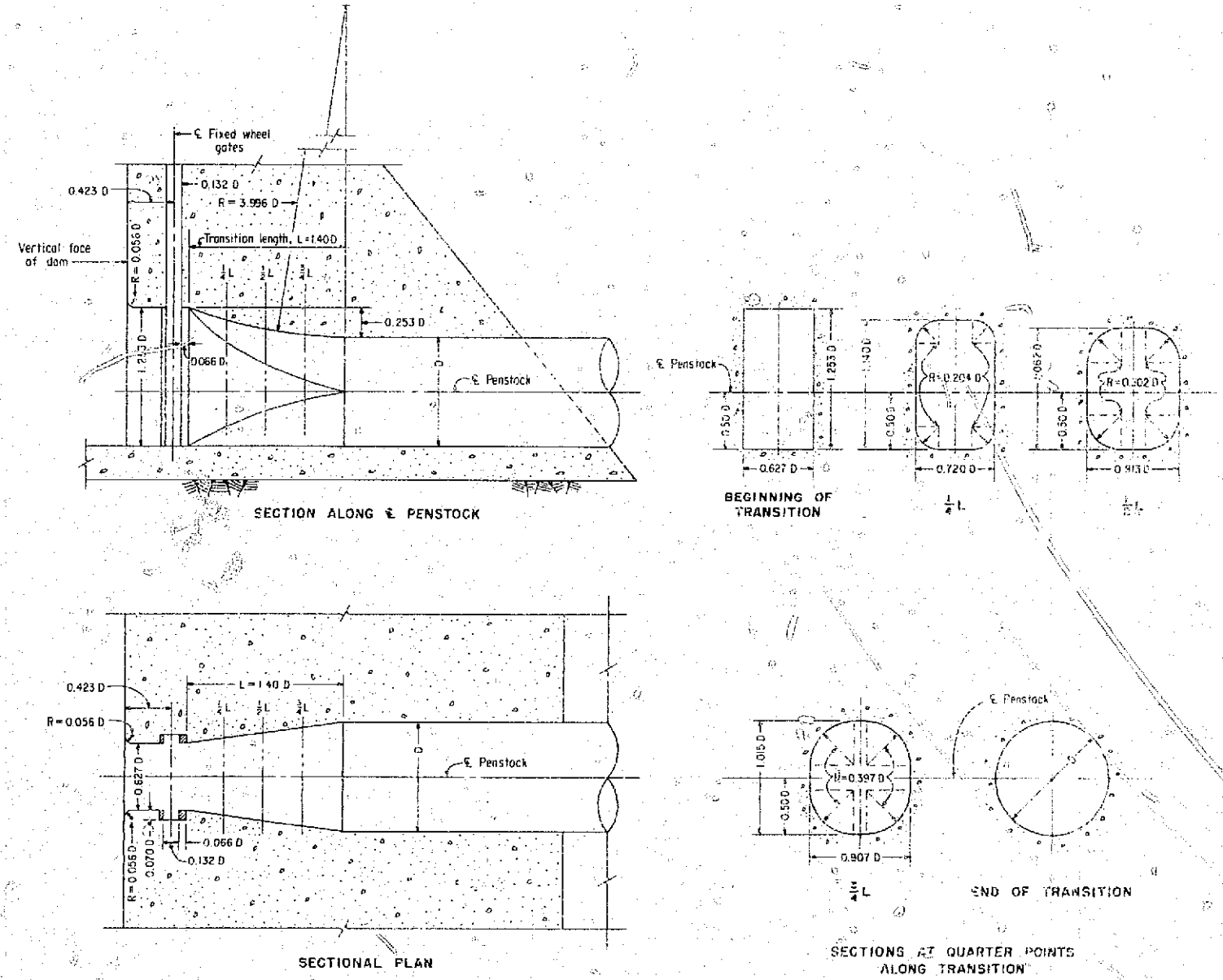

Figure 3. Initial entrance.

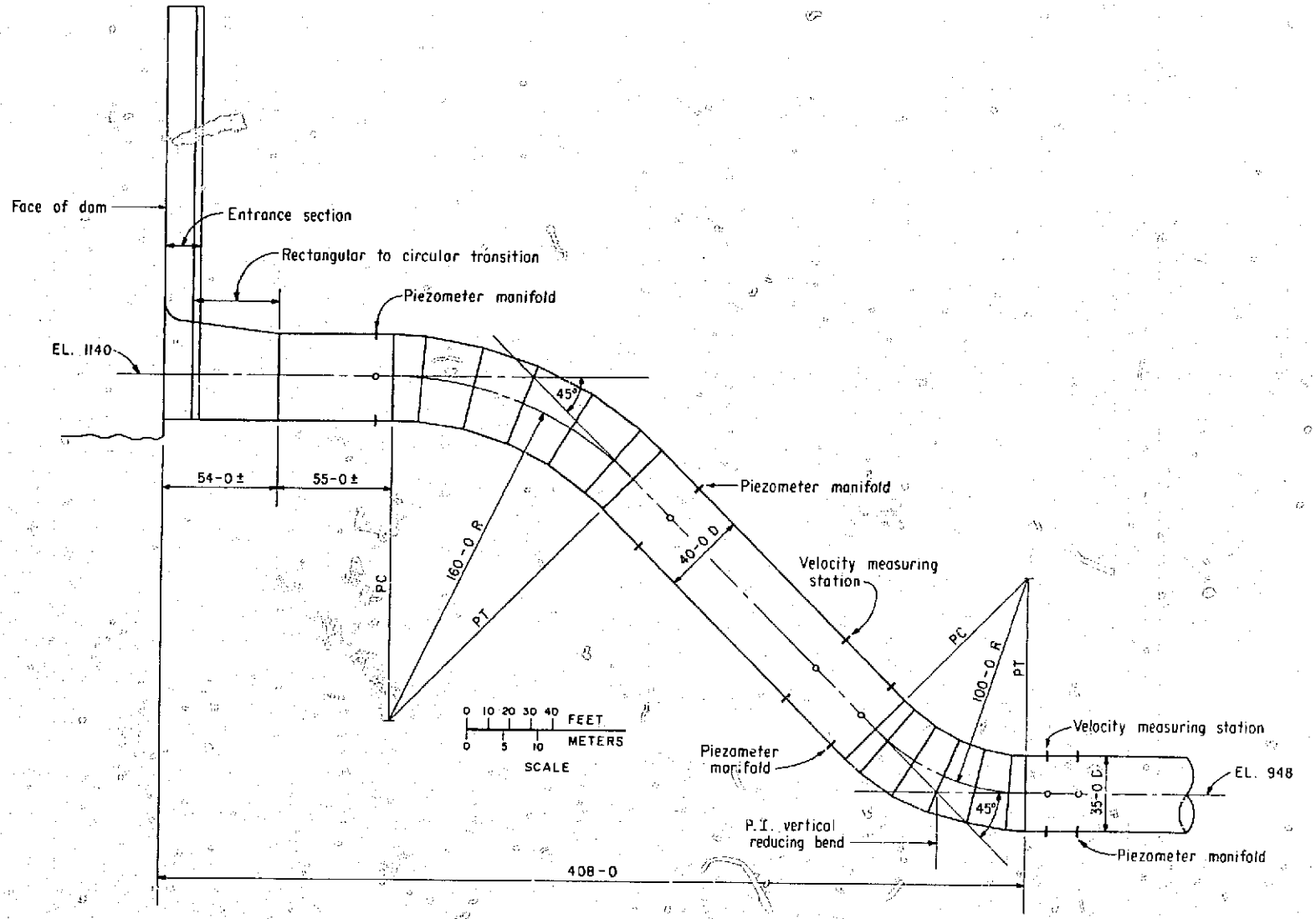

Figure 4. Penstock configuration.

gate section, and the rectangular-to-circular transition; no attempt was made to separate the form loss and the friction loss. Since the loss designated as the entrance loss was measured in a comparatively short length of the structure, it probably did not truly represent the total loss caused by this portion of the structure and should be considered a qualitative measurement used to compare various configurations. (Note: The loss is the reservoir elevation minus the sum of the piezometric elevation pressure head and velocity head at the downstream station.) For convenience the head loss has been converted to a loss coefficient by dividing the total loss by the velocity head (h_v) of the flow in the penstock. In turn, this coefficient has been related to the Reynolds number of the flow in the model penstock. The Reynolds number for the model ranged from 3.0×10^5 to 1.4×10^6. [Model discharge range 2.5 to 12.3 cfs (0.07 to .35 cu m/sec).]

For the initial structure, the head loss ranged from 0.325 h_v at the low Reynolds number to 0.190 h_v at the high Reynolds number. The steep slope of the loss coefficient curve indicated that the coefficient would probably become smaller if it had been possible to discharge a larger flow quantity through the model penstock.

The second measurement obtained to evaluate the entrance was the pressure distribution on the flow surfaces. Piezometers were located along the roof centerline and left side centerline from the P.T. of the entrance curve to a short distance into the rectangular-to-circular transition, Figure 5.

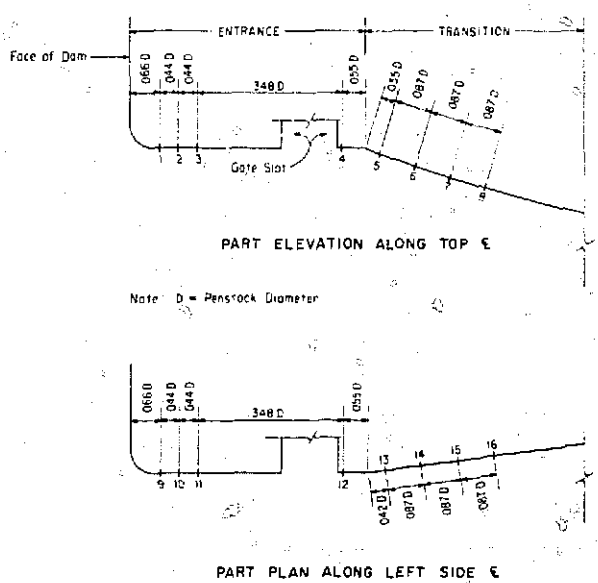

Figure 5. Piezometer locations, initial entrance.

The pressures have been converted to pressure drop coefficients, which is the drop from the reservoir elevation to the piezometer pressure head elevation divided by the velocity head of the flow in the penstock. The pressure drop coefficients for the initial entrance are shown on Figure 6. The curves show an extreme pressure drop on both the roof and side of the entrance. The pressure drop coefficient was about 2.4 at the downstream tangent point (P.T.) of the entrance curve and abruptly dropped to about 1.5 immediately downstream from the gate slot near the end of the rectangular section. The coefficients then gradually fell and leveled off at about 1.2 in the transition. The measurements indicated that the entrance curve was much too sharp and the flow might separate from the sidewalls at the entrance. A short distance downstream from the entrance (at the start of the rectangular-to-circular transition) the pressure drop coefficients decreased in value and eventually reflected the friction energy loss and change in velocity. The drop coefficient of 2.4 was equivalent to a pressure drop at the entrance of about 29 feet (8.8 meters) for normal penstock operation. Downstream where the curves had stabilized, the pressure drop was about 14-1/2 feet (4.4 meters) which is about the same as the sum of the measured friction energy loss between the two points and the velocity head in the penstock.

Observations were made to determine the reservoir elevation at which vortices would be likely to appear

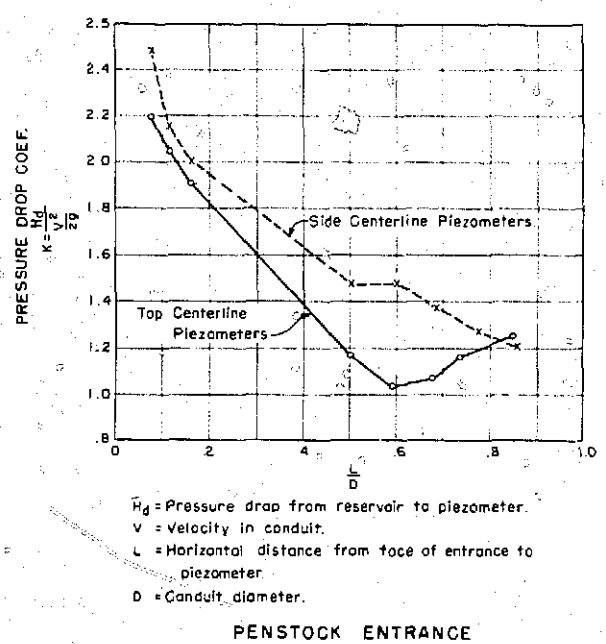

Figure 6. Pressure drop coefficients, initial design.

over the entrance. For these observations, a discharge of about 50,000 cfs (1,400 cu m/sec) was used. This flow produced a model velocity of about 6.2 ft/sec (1.8 m/sec) equivalent to a prototype velocity of almost 40 ft/sec (12 m/sec). [The design flow had not been finalized at the time of these initial studies and was eventually set at 34,850 cfs (986 cu m/sec), giving a flow velocity of about 27.7 ft/sec (8.4 m/sec) in the penstock.] This test showed that the initial small swirls appearing over the entrance at reservoir elevation 1262 [122 feet (37.2 meters) above the entrance centerline] developed into constant strong (well-formed) vortices when the reservoir fell to elevation 1239.

Maximum reservoir water surface will be at elevation 1290 and minimum reservoir water surface will be 1208. The well-formed vortices that formed at elevation 1239 in the model suggest that air-entraining vortices could form in the prototype structure at or near the same reservoir elevation.

First modification.—The 2:1 height-to-width ratio was retained, but a bellmouth entrance curve with a compound radius replaced the simple radius of the initial entrance, Figure 7. In effect, the bellmouth entrance provided a more gradual increase in velocity for the flow entering the penstock. The more gradual convergence would be expected to reduce the head loss in the entrance and provide a more favorable pressure distribution on the flow surfaces.

The head loss coefficient ranged from about 0.103 at a Reynolds number of 3×10^5 to 0.138 at a Reynolds number of 1.4×10^6, a significant improvement over the initial entrance. The pressure distribution on the flow surfaces also showed a considerable improvement. On the roof centerline the pressure drop coefficient was about 1.0 at the entrance, reduced to about 0.6 near the start of the rectangular-to-circular transition, and then gradually increased to about 1.1 in the transition, Figure 8. The pressure distribution on the side centerline showed a slightly different trend. The pressure drop coefficients were about 1.3 at the entrance, slightly declined to 1.2 a short distance inside the entrance, and gradually increased to 1.3 at the start of the transition. In the transition the coefficients decreased to a minimum value of about 0.95 before starting an increase to about 1.15.

The vortex characteristics were slightly improved with this entrance. At the same test discharges used for the initial entrance, a very slight tendency (intermittent) for a vortex to form over the entrance was noted at reservoir elevation 1260, the same as noted previously. However, the strong, steady vortex did not appear until reservoir elevation 1230 was reached, about 9 feet (2.7 meters) lower than with the initial entrance.

Second modification.—The entrance curve was modified by adding modeling clay to provide a more abrupt curve, Figure 7. The curve thus formed was elliptical and formed a boundary about midway between the original entrance and the first modification. This method of modifying the entrance covered the piezometer openings, making it impossible to determine pressure distribution on the flow surfaces. However, the head loss coefficients were essentially unchanged from the first modification.

Third modification.—A more economical entrance was believed to be achievable if the height-width ratio was changed to 1-1/2:1. Also this would allow for greater

DIMENSION	CURVE 1	CURVE 2	CURVE 3	CURVE 4
X_1	132 D	10 D	.068 D	.056 D
X_2	357 D	262 D	181 D	.056 D
X_3	277 D	212 D	144 D	--
Y_1	179 D	131 D	089 D	.056 D
Y_2	122 D	087 D	061 D	--
R_1	132 D	10 D	066 D	056 D
R_2	70 D	532 D	40 D	--

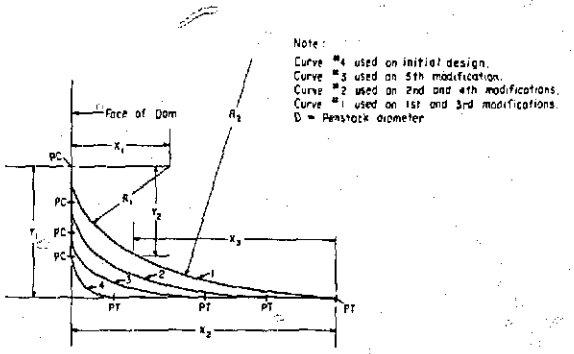

Figure 7. Comparison of portal curves.

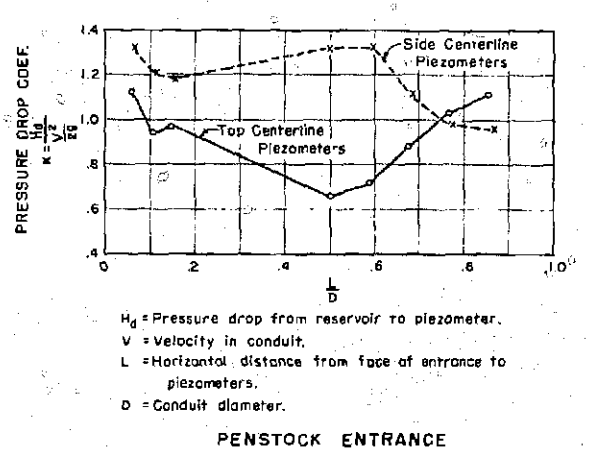

Figure 8. Pressure drop coefficients, first modification.

submergence at normal reservoir operating levels and thus should reduce the tendency for vortices to form, Figures 7 and 9.

The curves at the portal of this entrance were the same as for the first modification. The three tests used to evaluate this concept were head loss, pressure distribution, and vortex tendency.

The head loss measurement showed a significant improvement over the previous entrances. The head loss coefficient ranged from 0.083 at a Reynolds number of 3×10^5 to 0.126 at 1.4×10^6. At the higher Reynolds numbers, the coefficient curve appeared to be asymptotic, indicating that the head loss coefficient in the prototype structure would be close to 0.13.

The pressure distribution on the flow surfaces was about the same as with the first modification which had the same portal curve. The pressure drop coefficients obtained from the roof piezometers were between 1.2 and 1.3 near the portal, fell to about 0.9 near the gate slot, then gradually increased to about 1.1 in the rectangular-to-circular transition. The pressure drop coefficients along the sides were about the same near the portal but remained near the 1.2 to 1.3 value down to the transition, and dropped to just under 1.0 in the transition, Figure 10.

With this entrance there was a slight intermittent tendency for a vortex to form between reservoir elevation 1250 and 1255. A strong, fairly consistent vortex did not form until the reservoir water surface dropped to elevation 1230, about the same as with the first modification.

Fourth and fifth modifications.—Modeling clay was placed on the entrance curves to form the same entrance shape as in the second modification. Head loss coefficients were virtually unchanged from those obtained from the third modification. No pressure distribution or vortex characteristic tests were performed.

Additional modeling clay was added to the entrance curves to form a curve that was approximately midway between the original curve and that used for the second and fourth modifications, Figure 7. The head loss coefficients increased and now ranged from 0.10 at low Reynolds number to 0.16 at the high Reynolds number. The coefficient obtained at the high Reynolds number indicated a prototype loss nearly as large as would be obtained with the original entrance.

Recommended Entrance Studies

The preliminary tests had shown that the penstock entrance should have a height-to-width ratio of 1-1/2:1 and that the portal curve should have a compound radius. The entrance was redesigned incorporating these features but modifying the portal curve to include the stoplog guides and seat. In effect, the upstream end of the curves were cut off to allow a blockout for ultimate installation of the guides, Figure 11. The entrance had compound radius curves at the portal on all four sides. The upstream ends of the curves were cut off to allow for the stoplog guides. The guides were placed so that they would not protrude into an imaginary boundary that would be formed had the entrance curves been complete. It was believed that this alinement would cause less turbulence at the entrance. Another difference from the earlier entrances was that the approach channel had to be lowered 10 feet. This required a curve on the invert of the entrance.

The height-to-width ratio of the entrance was 1-1/2:1, and the area at the gate section was equal to the area of the penstock. The rectangular-to-circular transition downstream of the gate section was 40 feet long and was symmetrical about the vertical centerline, but the convergence of the roof toward the horizontal centerline was greater than the floor convergence. Four rows of piezometers were installed: right side centerline, top right corner, top centerline, and left side centerline. All features are shown in Figure 11.

Tests used in this part of the investigation included head loss measurements in the entrance, velocity distribution in the penstock downstream from the bends, pressure distribution on the entrance curve surfaces, dynamic variation of these pressures, turbulence measurements in the penstock, and a few tests to determine vortex characteristics.

Approach flow test conditions were with and without a trashrack at the entrance, and with the flow approaching the entrance from directly in front or approaching from the left side so that the flow turned nearly 90° to enter the penstock. The reason for having the flow enter from the side was to more nearly represent the true approach condition that will exist in the prototype structure. The earlier development tests had been made with the flow entering from in front; therefore, this test condition was also continued so as to have a direct basis for comparison with the previous

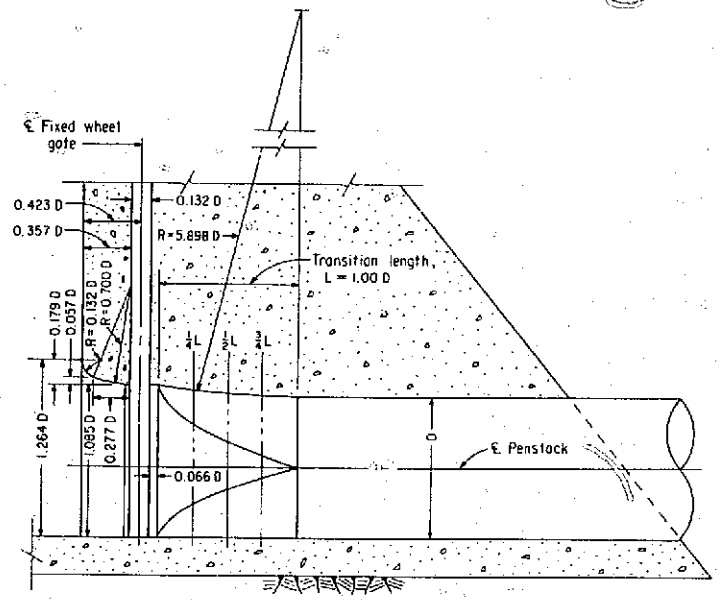

SECTION ALONG ℄ PENSTOCK

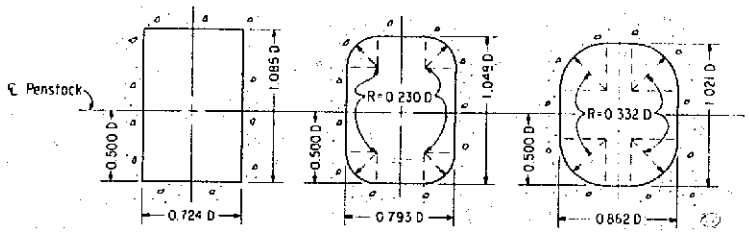

BEGINNING OF TRANSITION ¼L ½L

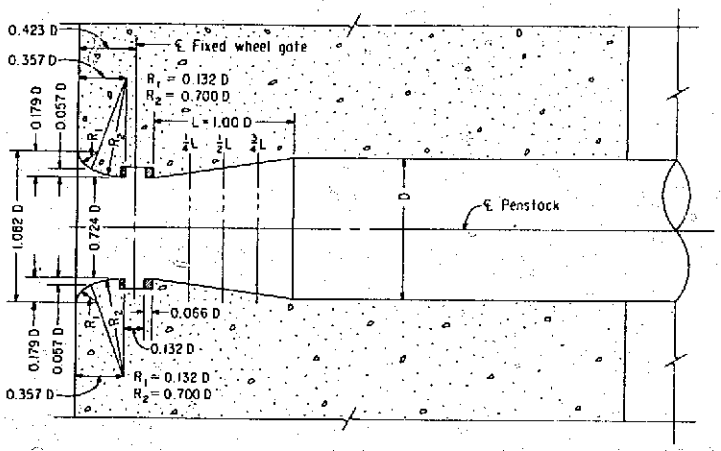

SECTIONAL PLAN

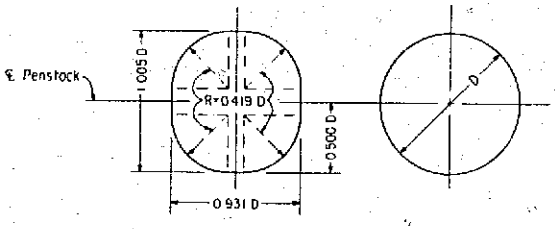

¾L END OF TRANSITION

SECTIONS AT QUARTER POINTS ALONG TRANSITION

Figure 9. Third modification.

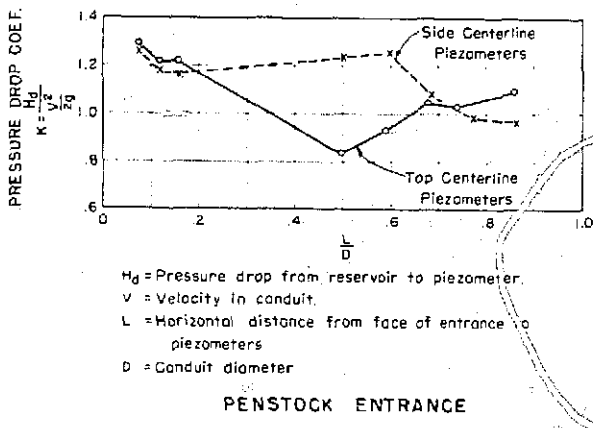

Figure 10. Pressure drop coefficients, third modification.

designs. Not all tests were made with all the possible combinations of these approach conditions.

Head loss coefficient.—The head loss coefficient for this configuration, that is, with the flow approaching from the front and no trashrack, was 0.08, Curve 1 on Figure 12. This was a considerable improvement over the previous test. Apparently, eliminating the upstream end of the curve was more than compensated by placing the streamlined curve on the invert. When the trashrack was installed the loss coefficient increased to 0.125 (Curve 2). Loss coefficients were not obtained with flow approaching from the side.

Pressure drop coefficients.—The effect of the flat surface at the upstream end of the curve was apparent in the pressure distribution. In the top right corner the piezometer at the start of the curve indicated a pressure drop coefficient of 1.2, and at the second piezometer (one-half inch downstream) the drop coefficient increased to 1.9, Figure 13. The top centerline piezometers showed the same tendency, that is, a coefficient of 1.2 at the first piezometer and 1.4 at the second piezometer. The coefficients remained high in the corner, and at the centerline the coefficients gradually reduced to below unity, Figure 13. The piezometers on the right side centerline registered a pressure drop coefficient of 1.6 at the first piezometer and gradually dropped to near 1.0 in the transition.

When the flow approached from the left side and all was diverted into the penstock, the top centerline piezometers showed an increase in the pressure drop coefficient to 2.5 at the first piezometer, gradually reduced to less than 0.8 at the start of the transition, and then showed a sudden increase to 2.3 in the transition. Pressure drop coefficients at the right side piezometers were the same as with symmetrical approach flow, but the pressure drop coefficients along the top right corner were only 0.8 at the first piezometer and increased to 1.3 a short distance downstream, Figure 13.

Measurements were also made with flow approaching from the side and maximum discharge diverted into the penstock and an equal discharge allowed to flow past the penstock entrance where it was diverted into a bypass line, which simulated flow through more than one penstock. This approach flow condition did not significantly affect the pressure distribution in the entrance except along the right side, Figure 13. The pressure coefficients along the right side centerline were only 0.8 at the upstream end, dropped to 0.6 a short distance downstream, and then increased to 1.0 The low pressure coefficients indicated that the flow impinged on the wall in this area. The force of the impingement was not sufficient to be of concern, however.

Pressure fluctuations.—Instantaneous pressure fluctuations were also measured at most of the piezometers that had been used to obtain the pressure coefficients. The pressure fluctuations indicate the degree of turbulence along the flow boundaries and whether instantaneous pressures exist that might be significantly above or below an average pressure.

For all three approach flow conditions and at all piezometers, the total pressure fluctuation was between 6 and 24 inches (15 and 60 cm) of water (prototype value). The greatest fluctuation always occurred at the roof centerline piezometers and was between 12 and 24 inches (30 and 60 cm) of water. The frequency of fluctuation was about 1 hertz. The fluctuation pattern was very regular with the symmetrical approach flow but was uneven or irregular for the two asymmetrical approach flow conditions.

Velocity distribution in penstock.—Tests were made to determine the velocity distribution in the penstock for both symmetrical and asymmetrical approach flow. The velocity distribution was not obtained with part of the flow bypassing the entrance. Because of the physical limitations of the model, it was not possible to measure the velocity distribution between the entrance and the upper vertical bend. The velocity distribution was obtained from vertical, horizontal, and diagonal traverses with a pitot cylinder at stations 40 feet upstream and downstream from the lower vertical bend. The pitot cylinder measurements were converted to the equivalent prototype velocities which were used to draw the isovel diagrams shown on Figure 14.

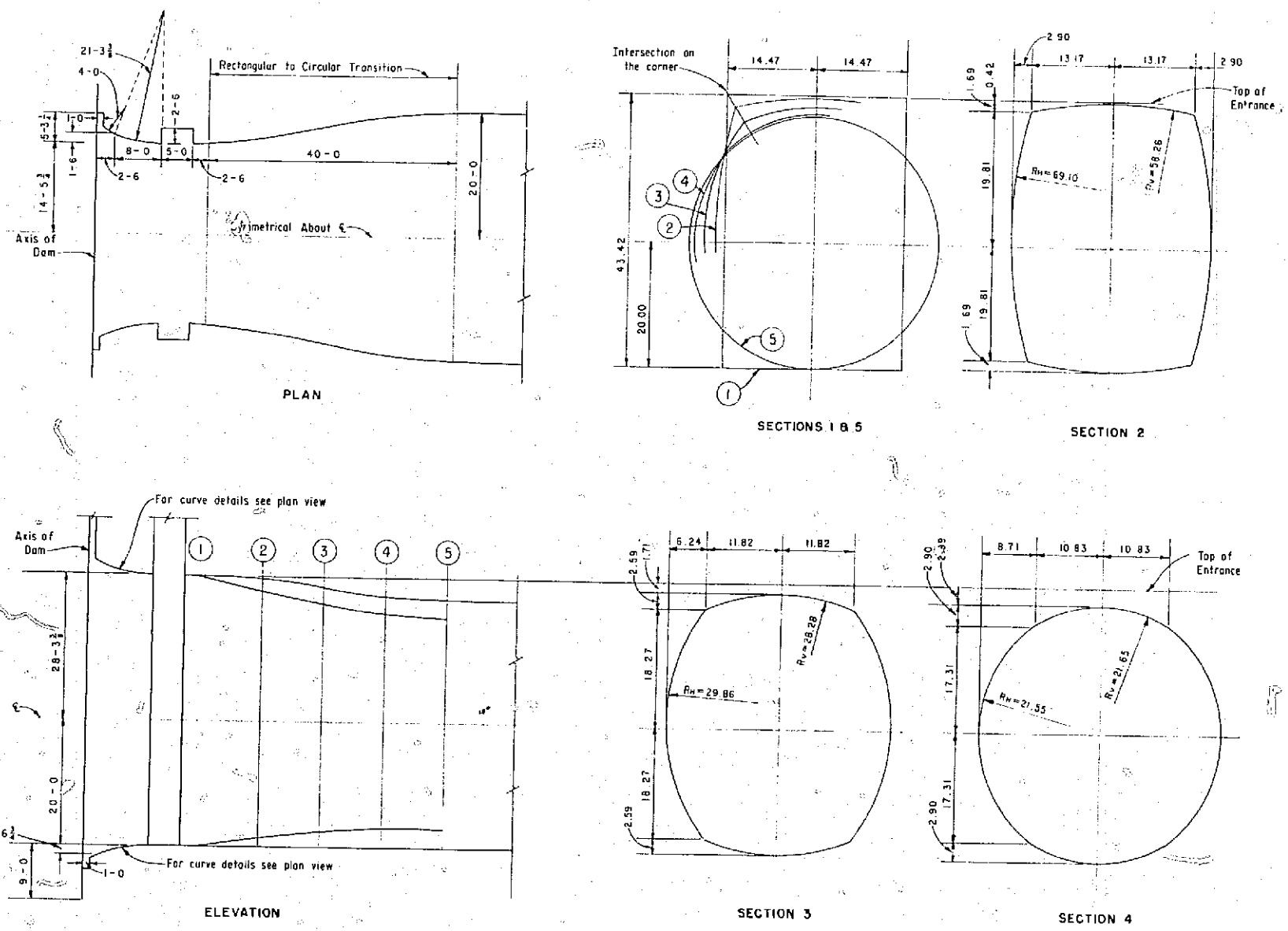

Figure 11. Final entrance and transition.

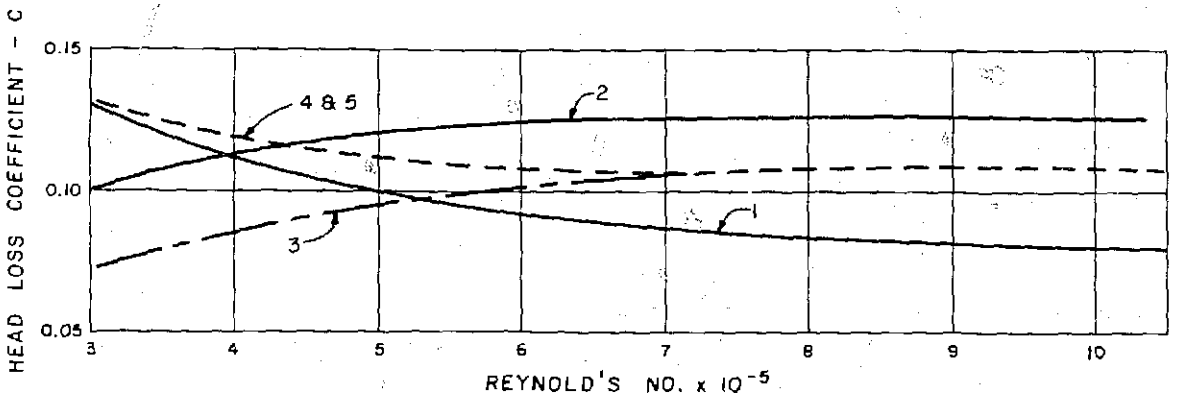

Head Loss = $C\frac{v^2}{2g}$

V = Velocity in 40'-Dia. penstock.

A. Symmetrical Entrance
   Symmetrical Approach Flow
   1. No trashrack
   2. With trashrack
B. Unsymmetrical Entrance
   Symmetrical Approach Flow
   3. No trashrack
   4. With trashrack
   Unsymmetrical Approach Flow
   5. No trashrack

Figure 12. Entrance head loss.

The distance between the penstock entrance and the velocity traverse station in the penstock and the fact that the flow went through the upper bend no doubt had some effect on the velocity pattern. However, it was felt that a comparison of the two isovel diagrams would show any effect of the approach flow conditions. The velocity distribution with the symmetrical approach flow showed that flow near the crown was at a slightly higher velocity than the average velocity, and in the lower left quadrant the velocity was slightly below average. The higher velocity near the crown and reduced velocity near the invert could be the result of the centrifugal effect of the flow going around the bend. There is no apparent explanation for the slight asymmetry of the low velocity area.

With the asymmetrical approach flow the velocity distribution in the penstock was better than it had been with the symmetrical approach flow. There was still a tendency for a higher velocity on the right side, but it was not as pronounced as in the previous test. Downstream from the lower bend, the velocity distribution in the penstock was very symmetrical except for a slight tendency toward lower velocity in the crown caused by the centrifugal effect of the flow going around the bend, Figure 14.

Turbulence measurements.—Although the velocity distribution had not indicated excessive flow asymmetry along the boundaries of the penstock, measurements were made to determine whether there was turbulence or flow asymmetry in the flow not adjacent to the boundaries. These measurements were made by placing a pressure transducer on the total (impact) head line of the pitot cylinder and recording the pressure fluctuations on an oscillograph. The fluctuations were obtained along the same traverses used for the velocity distribution measurements. The oscillograph recordings are shown in the appendix, Plates 1 to 8.

A description of the oscillographs follows:

(1) [Symmetrical approach flow—40-foot (12.2-meter) diameter conduit].—On the horizontal traverse pressure fluctuations were noticeable but not considered extreme; magnitude was equivalent to about 1.5 feet (0.46 meter) of water at a frequency of about 2 hertz. The fluctuations were about the same across the full width of the conduit. The vertical traverse showed very slight pressure fluctuations, less than a half foot (15 cm) in magnitude at the same frequency as the horizontal traverse. In the diagonal traverse from left to right, the magnitude and frequency of the pressure fluctuations were about the same as for the horizontal traverse and were also the same across most of the conduit except for a section just below

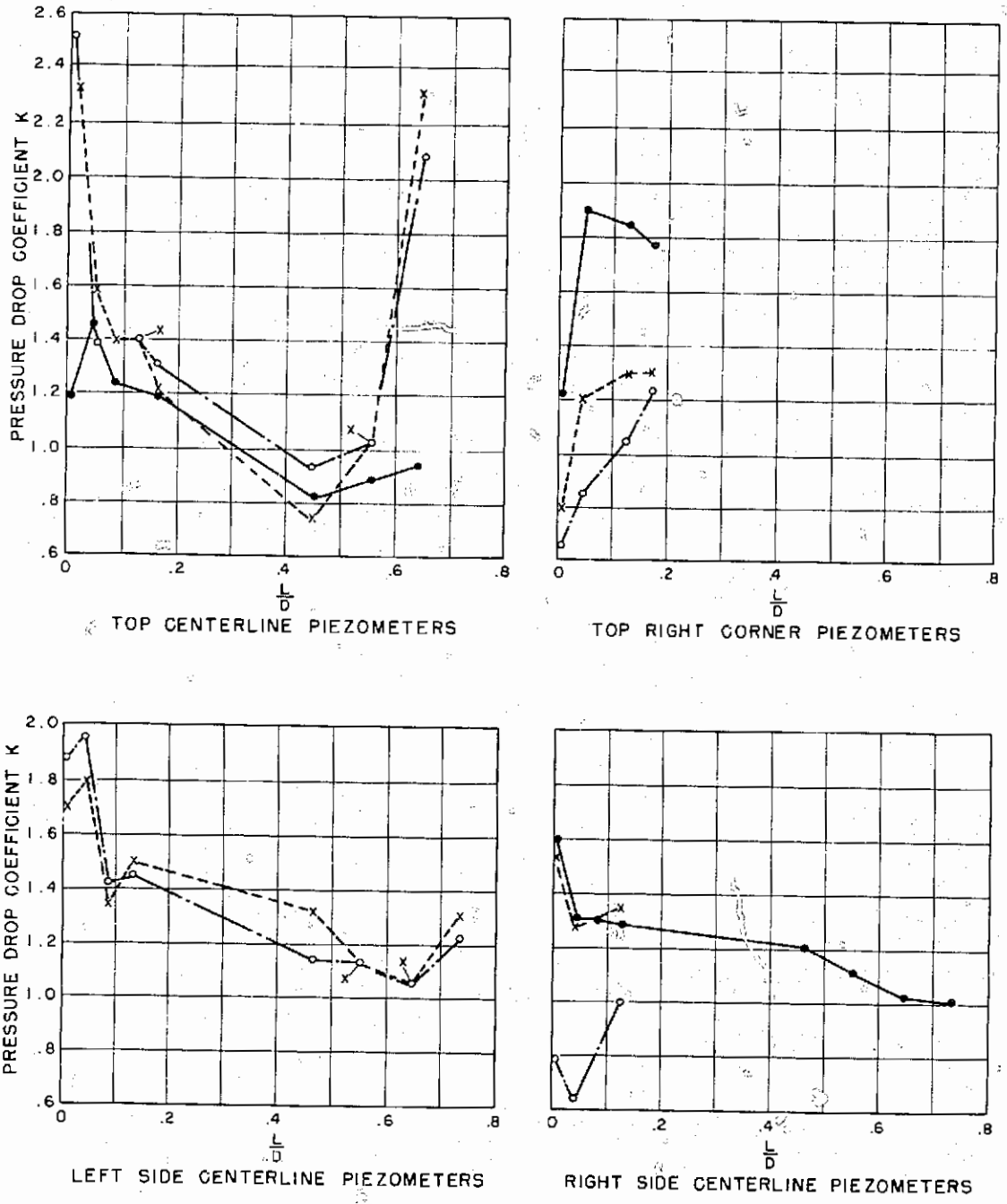

$K = \frac{H_d}{\frac{V^2}{2g}}$ where H_d = Pressure drop from reservoir to piezometer and V = Velocity in penstock.

L = Horizontal distance from face of entrance. D = Penstock diameter.

●——● Symmetrical approach flow.

×– – –× Unsymmetrical approach flow - all flow enters penstock.

○—·—○ Unsymmetrical approach flow - half of flow enters penstock, half of flow bypasses penstock.

PENSTOCK ENTRANCE

Figure 13. Recommended design, pressure distribution.

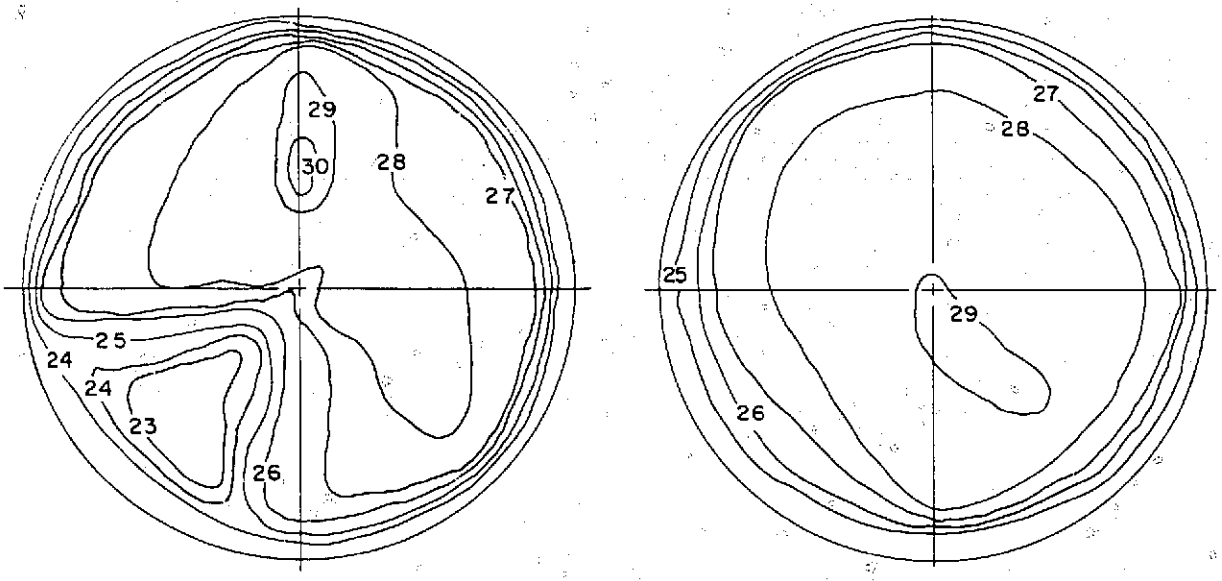

A. SYMMETRICAL APPROACH FLOW B. UNSYMMETRICAL APPROACH FLOW

40-FT. DIAMETER PENSTOCK-40-FT. UPSTREAM FROM P.C. OF LOWER BEND. AVERAGE VELOCITY = 27.7 FT./SEC.

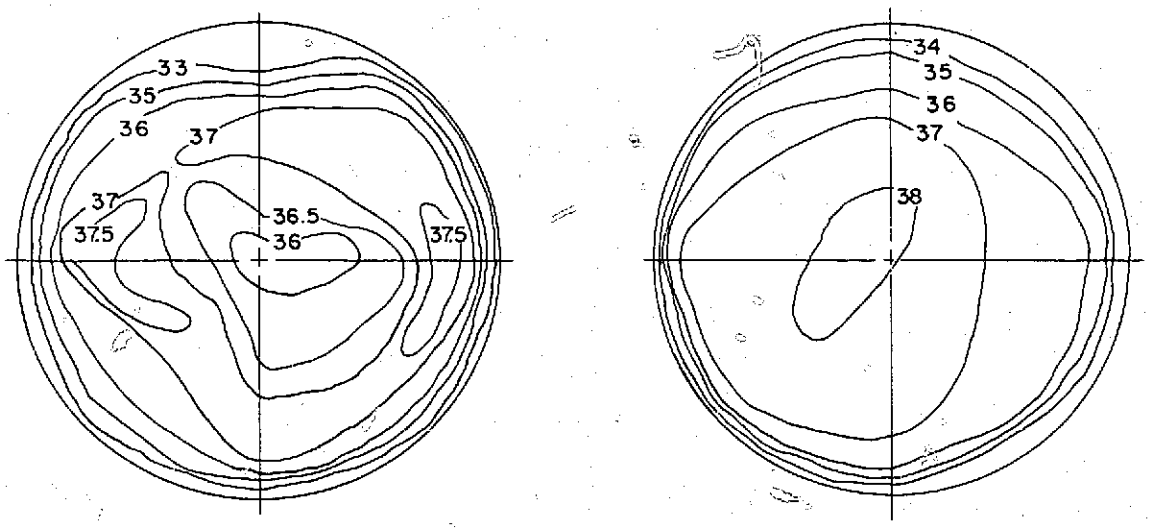

C. SYMMETRICAL APPROACH FLOW D. UNSYMMETRICAL APPROACH FLOW

35 FT. DIAMETER PENSTOCK-40-FT. DOWNSTREAM FROM P.T. OF LOWER BEND. AVERAGE VELOCITY = 36.2 FT./SEC.

Figure 14. Velocity distribution in penstock, recommended design.

and to the right of the center where the magnitude increased to about 2.5 feet (0.76 meter) of water. The pressure fluctuations on the right-to-left diagonal traverse were very similar in both magnitude and frequency to those obtained from the vertical traverse. These measurements indicated that there was more turbulence in the flow in the lower part of the upper left quadrant and upper part of the lower right quadrant when the approach flow was symmetrical.

(2) [Symmetrical approach flow—35-foot (10.7-meter) diameter conduit].—In the 35-foot-diameter conduit downstream from the lower bend, there were no turbulent areas except for a small section near the crown of the conduit along the vertical traverse.

(3) [Asymmetrical approach flow—40-foot (12.2-meter) diameter conduit].—On the horizontal traverse the turbulence was about the same as had been determined with the symmetrical approach flow. The vertical traverse indicated good flow conditions over the top two-thirds, but in the lower one-third, extreme turbulence was encountered. The magnitude of the pressure fluctuations was in the order of 3 feet (0.91 meter) of water at a frequency of about 2 hertz. Pressure fluctuations along the left-to-right diagonal traverse were negligible. Along the right-to-left diagonal traverse, pressure fluctuations in the order of 2 to 2.5 feet (0.61 to 0.76 meter) were measured.

With the asymmetrical approach flow, two areas of turbulence were noted; the entire lower left quadrant had turbulent flow conditions, and the lower half of the upper right quadrant showed turbulent conditions.

(4) [Asymmetrical approach flow—35-foot (10.7-meter) diameter conduit].—In the 35-foot-diameter conduit the turbulent area covered the entire upper right quadrant. The pressure fluctuations were particularly violent near the crown along the centerline. Flow in the remaining portion of the conduit at this section was very stable.

Summary of tests.—Generally speaking, flow conditions in the penstock with the recommended entrance were satisfactory. Some operating conditions gave rise to concern about the overall effectiveness, especially for asymmetrical approach flow. These are summarized below:

(1) Head loss coefficient.—The head loss coefficient increased from 0.080 with symmetrical approach flow to 0.125 with asymmetrical approach flow.

(2) Pressure drop coefficient along surface curves of the entrance.—On the top centerline the pressure drop coefficient increased from 1.4 with symmetrical approach flow to 2.4 with asymmetrical approach flow.

(3) Turbulence in penstock.—With asymmetrical approach flow the degree of turbulence increased, and there were more turbulent areas.

In the tests for dynamic pressures along the entrance curve surfaces and velocity distribution in the penstock, very little difference was noted between symmetrical and asymmetrical approach flow.

Flared Entrance Studies

It was thought that if the entrance curves were flared along the crown and along the left side toward the direction from which the asymmetrical approach flow originated, some of the adverse flow conditions might be alleviated. To determine this, a new entrance was constructed. The 1-1/2:1 height-to-width ratio, the area at the rectangular section (gate section) equal to the penstock area, and the compound radius entrance curves on the right side and invert were retained. The only change was to use a simple radius for the entrance curves on the crown and left side, Figure 15.

Tests used to evaluate this concept were: (1) the entrance head loss; (2) pressure drop along the entrance curves; (3) dynamic pressures along the entrance curves; (4) velocity distribution in the penstock; and (5) turbulence measurements in the penstock.

Entrance head loss.—The entrance head loss coefficient with symmetrical and asymmetrical approach flow was 0.109 compared to 0.080 for the symmetrical approach and 0.125 for the asymmetrical approach obtained with the symmetrical entrance, Figure 12 (Curves 3, 4, and 5). The improved loss coefficient with asymmetrical approach flow showed that flaring the entrance in the direction of the approach flow allowed the water to enter smoothly, creating very little turbulence.

Pressure drop coefficients.—With symmetrical approach flow there was very little change in the magnitude of the pressure drop coefficients. In some cases the high

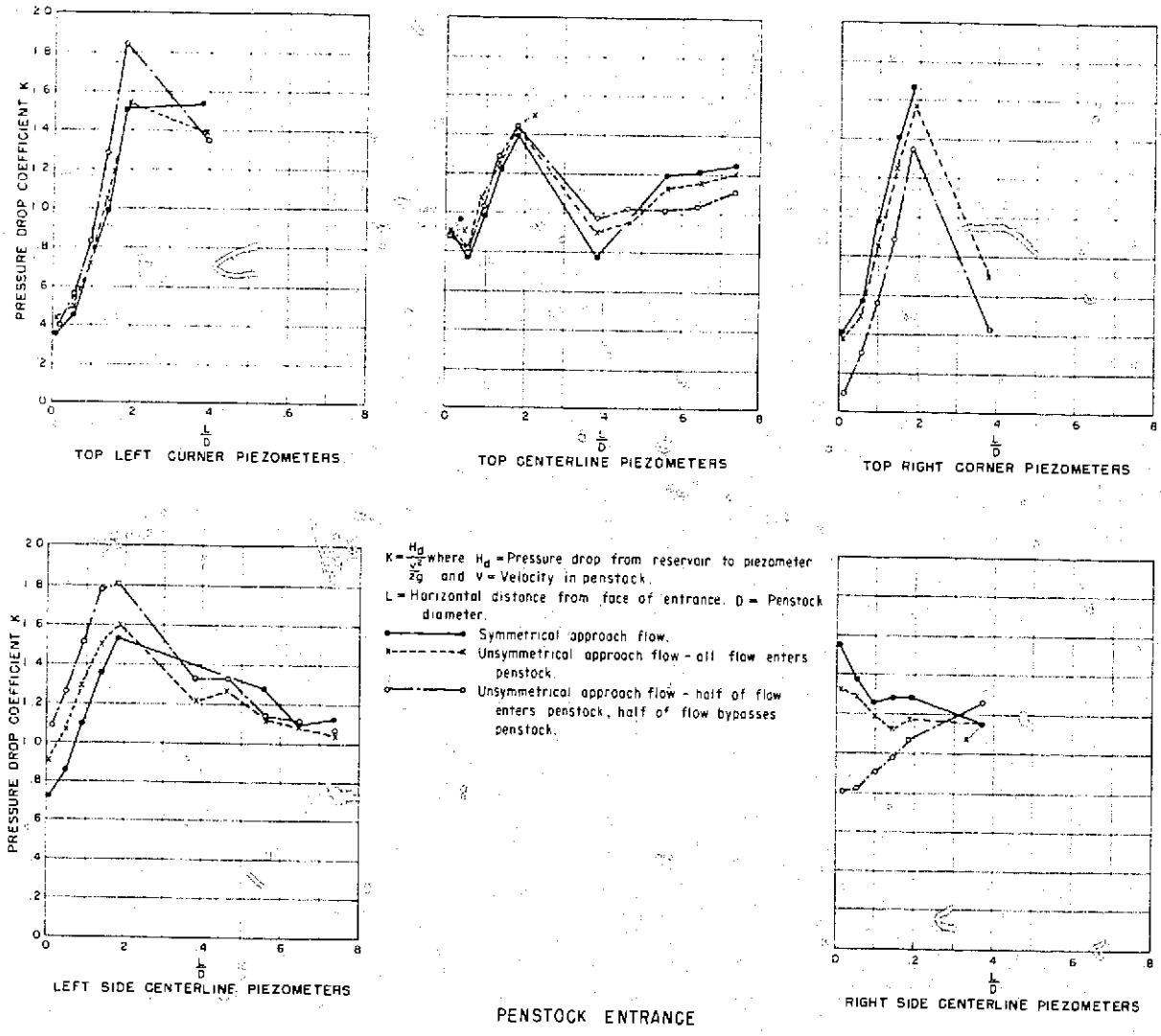

Figure 16. Flared entrance, pressure distribution.

two entrances for the asymmetrical approach condition. For four of the five evaluation points (head loss, pressure drop coefficients, pressure fluctuation on surfaces, and velocity distribution in penstock) the flared entrance proved slightly more advantageous. The fifth evaluator (turbulence in penstock) was much worse with the flared entrance, particularly in the 35-foot (10.7-meter) diameter section. It was felt that turbulence at the entrance to the scrollcase would adversely affect the turbine operation and that the best possible scrollcase entrance conditions should be used. Also, the flared entrance would require larger and heavier stoplogs to span the wider opening. The expense of the larger stoplogs would probably more than offset the cost savings derived from the lower head loss coefficient. Based on these two criteria, the symmetrical entrance as shown on Figure 11 was used for the prototype installation.

Trashrack Studies

A scale model of the proposed trashrack design was constructed for the penstock entrance, Figure 18. The model represented to scale, the width, length, and spacing of all the bars and structural members.

The following observations were made to determine the effect of the trashrack in front of both the symmetrical and flared entrance with symmetrical approach flow.

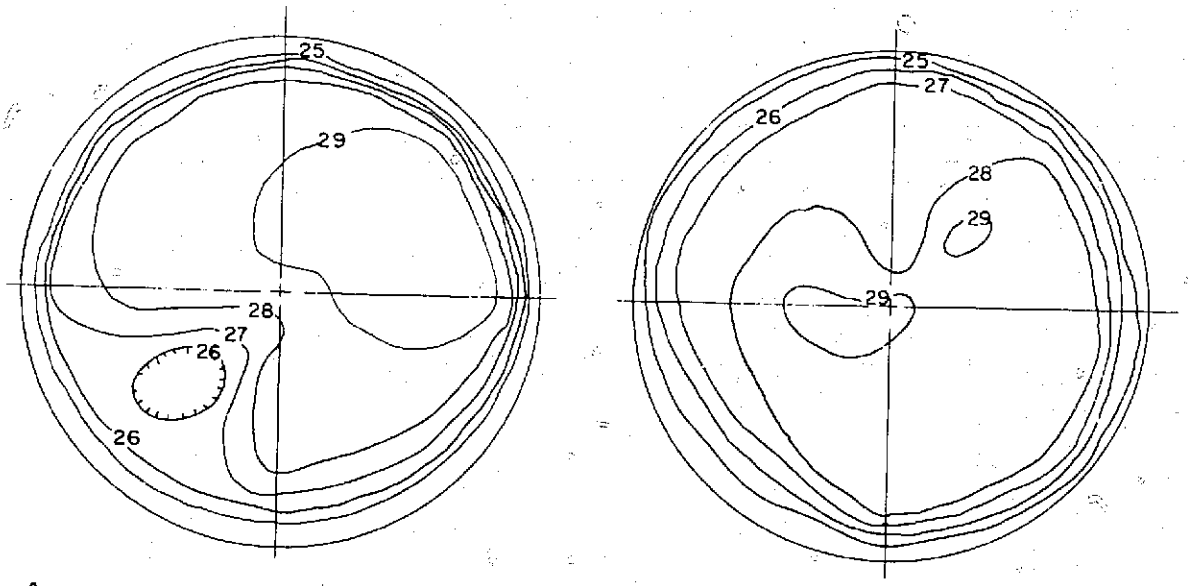

A. SYMMETRICAL APPROACH FLOW B. UNSYMMETRICAL APPROACH FLOW

40-FT. DIAMETER PENSTOCK-40-FT. UPSTREAM FROM P.C. OF LOWER BEND. AVERAGE VELOCITY = 27.7 FT./SEC.

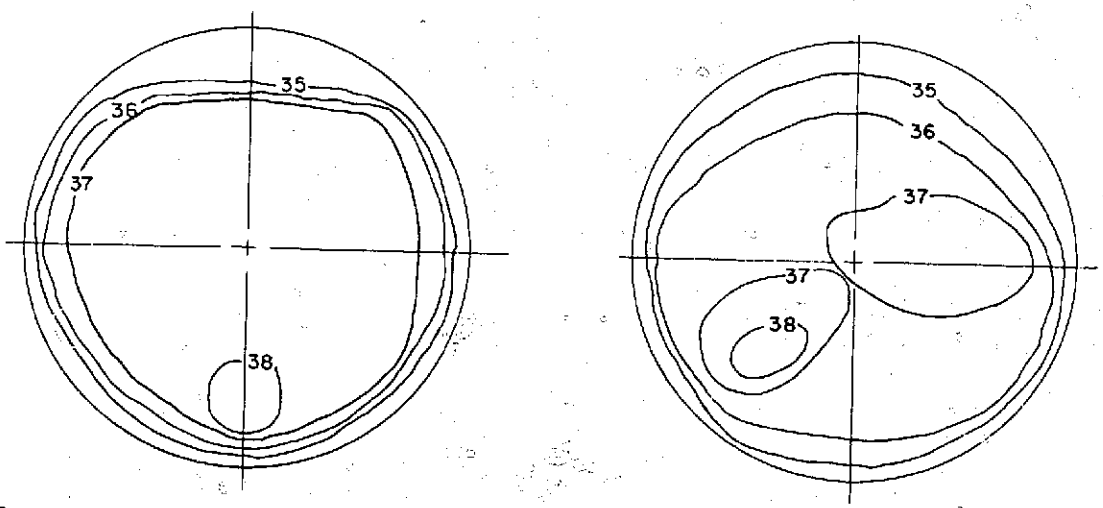

C. SYMMETRICAL APPROACH FLOW D. UNSYMMETRICAL APPROACH FLOW

35 FT. DIAMETER PENSTOCK-40-FT. DOWNSTREAM FROM P.T. OF LOWER BEND. AVERAGE VELOCITY = 36.2 FT./SEC.

Figure 17. Velocity distribution in penstock, flared entrance.

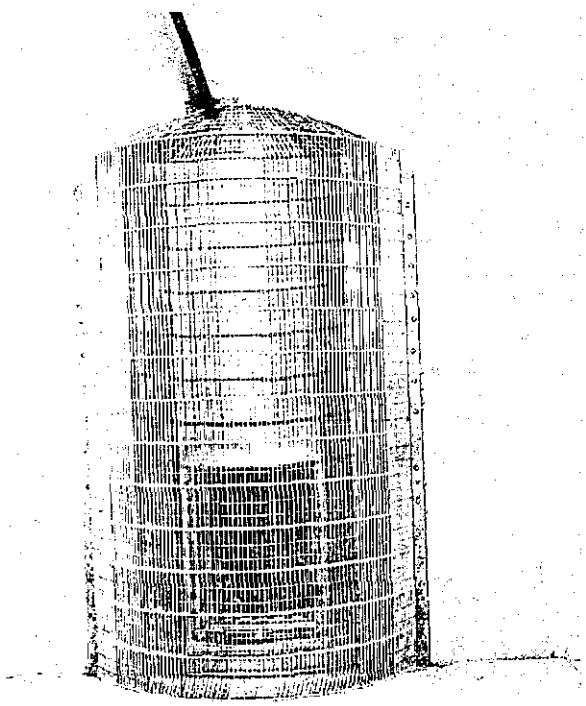

Figure 18. Trashrack in front of penstock entrance. Photo P1222-D-74686

Head loss coefficient.—The trashrack increased the loss coefficient for the symmetrical entrance from 0.080 to 0.125. The trashrack did not change the head loss coefficient for the flared entrance.

Pressure drop coefficient.—The trashrack did not affect the pressure drop coefficients for the flared entrance. This observation was not made with the symmetrical entrance.

Velocity distribution.—(This comparison was made with only the flared entrance.) The trashrack seemed to make minor changes in the velocity distribution in the penstock, Figure 19. For the 40-foot (12.2-meter) diameter section, the elevated and reduced velocity areas rotated about 30° counterclockwise; in the 35-foot (10.7-meter) diameter section, a reduced velocity core formed in the center of the section. Even with these anomalies the velocity distribution was excellent.

Conclusions.—The trashrack will increase the head loss through the structure and tend to smooth out some flow irregularities in the penstock.

Bend Studies

Both the upper and lower elbows of the penstock were studied in the model. The upper elbow has a 45° vertical bend with a 160-foot (48.8-meter) radius. The degree of curvature and radius of the upper elbow had been fixed by structural and construction considerations and would not be changed unless the hydraulic investigations showed that they were entirely inadequate. However, both the degree of curvature and radius of curvature were considered to be conservative; subsequent tests confirmed this.

The configuration of the lower elbow was not restricted by these considerations, so three different elbows were tested to determine the most efficient and economical combination, Figure 20. The penstock from the intake at the reservoir to the lower elbow was 40 feet (12.2 meters) in diameter. The entrance to the scrollcase approximately 20 feet (6.1 meters) downstream from the P.T. of the lower elbow was 35 feet (10.7 meters) in diameter. A means of reducing the penstock diameter was included in the lower elbow design. The three elbows tested were a 45°, 140-foot (42.7-meter) radius with the penstock diameter reducing from 40 to 35 feet; a 45°, 100-foot (30.5-meter) radius with the penstock diameter reducing from 40 to 35 feet; and a 45°, 100-foot radius constant 40-foot diameter, followed by a 20-foot-long cone to reduce the penstock diameter to 35 feet.

Two tests were used to evaluate the lower bend. One was to measure the velocity distribution at the P.C. of the bend and 35 feet (one diameter) downstream from the P.T. of the bend. The second test was to determine the energy loss between the same two points.

The velocity distribution was obtained by making vertical, horizontal, and diagonal velocity traverses across the penstock and plotting isovels from these data. The energy loss was obtained by subtracting the sum of the measured pressure head and the computed velocity head at the downstream station (P.T.) from the sum of the measured pressure head and the computed velocity head at the upstream station (P.C.). For purposes of comparison, the loss has been expressed as a loss coefficient, K, which is the energy loss divided by the velocity head in the 40-foot-diameter conduit. The head loss measurements were obtained for model Reynolds number range between 3×10^5 and 1.1×10^6. The Reynolds number for prototype operation will be approximately 1×10^8, but the model studies showed that the head loss

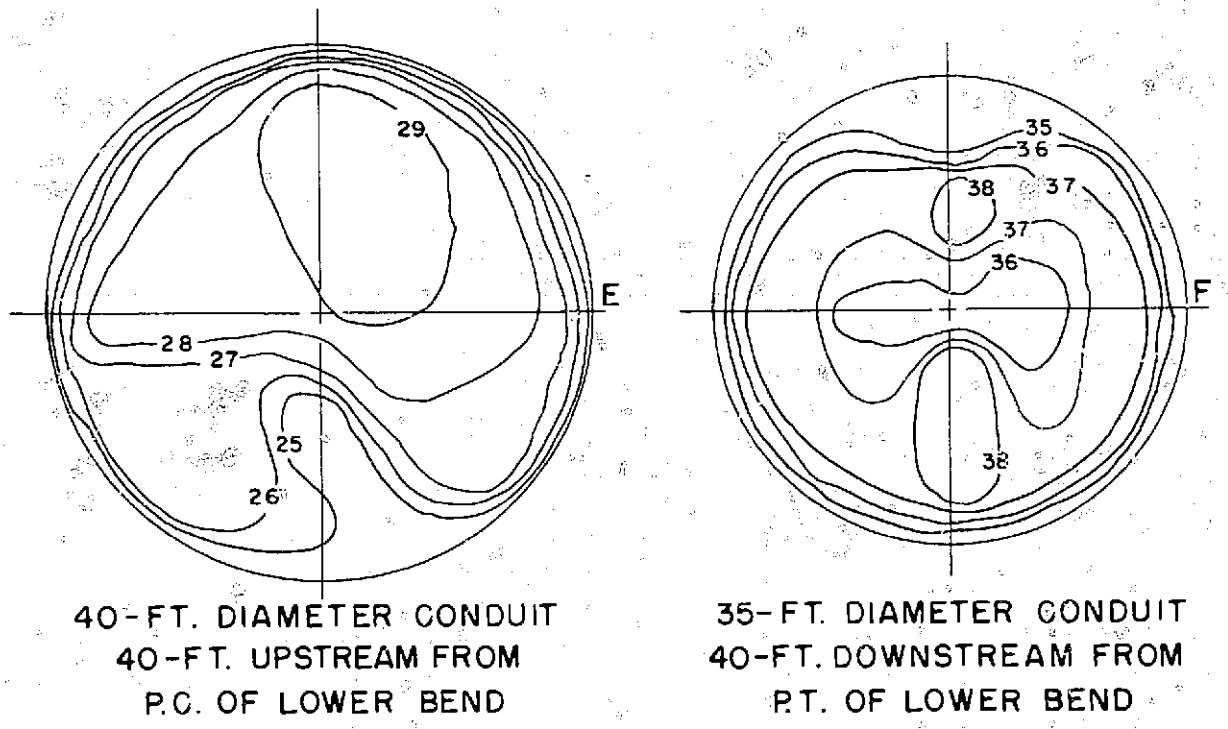

Figure 19. Effect of trashrack on velocity distribution.

coefficients did not change significantly for Reynolds numbers greater than 5×10^5. In determining the loss coefficients the friction loss was not separated from the total loss.

Upper bend.—The velocity distribution upstream and downstream of the upper elbow was not determined; however, the velocity distribution upstream of the lower elbow indicated that the flow was not excessively upset by the upper elbow, Figure 21. The velocity near the crown of the penstock was slightly higher than in the invert, which would be expected as a result of the centrifugal force of the flow going around the bend. Also, the velocity in the lower left quadrant was 4 to 5 feet (1.2 to 1.5 meters) per second lower than in the lower right quadrant.

The energy loss caused by the upper elbow was 0.08 velocity head, typical for a 45° elbow with this radius of curvature (0.03 velocity head for friction loss and 0.05 velocity head for bend loss).

Lower bends—energy loss.—The energy loss coefficients were essentially the same for the three configurations tested. The loss coefficient varied from 0.10 for the 100-foot (30.5-meter) radius elbow with conical reducing section to 0.11 for both the 100-foot-radius and 140-foot (42.7-meter) radius reducing diameter elbows. These loss coefficients were not excessive and indicated that the three configurations would be equally satisfactory.

Velocity distribution.—The three elbow configurations gave almost the same velocity distribution at the downstream entrance to the scrollcase, Figure 21. The 140-foot-radius reducing diameter elbow and the elbow with the reducing cone showed a very minor higher velocity in the lower right quadrant, and the 100-foot-radius reducing diameter elbow showed a very small low velocity area in the center. All three configurations indicated a lower velocity at the crown and higher velocity on the invert due to the centrifugal force of the flow going around the bend.

The model studies indicated no apparent advantages for any one of the elbows. The 100-foot-radius reducing diameter elbow was selected for prototype installation.

Small Entrance Studies

The hydraulic characteristics of the entrance were so satisfactory that it was thought a smaller entrance might prove adequate and would be more economical.

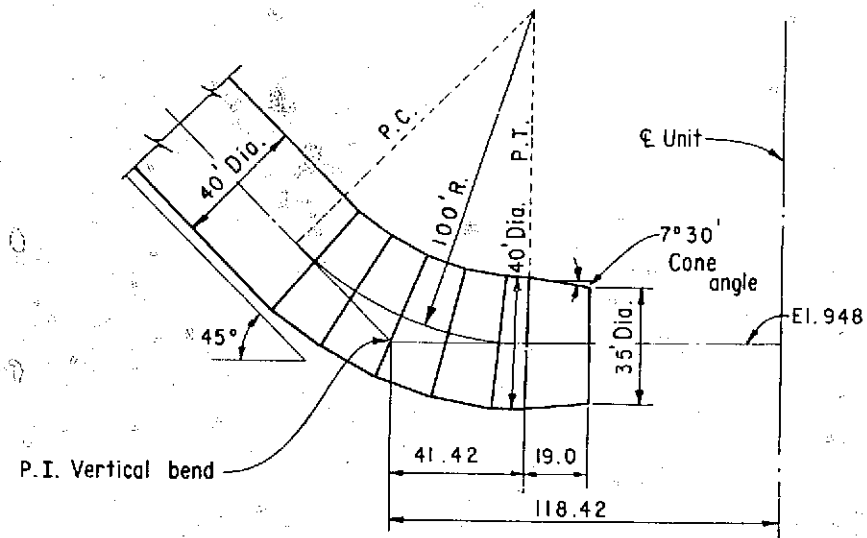

A. CONSTANT DIAMETER-REDUCING CONE

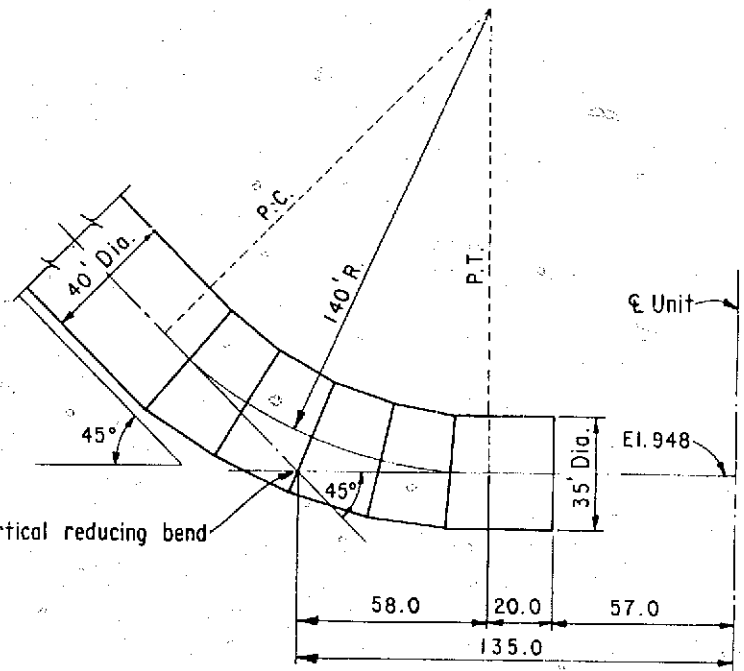

B. 140-FOOT RADIUS REDUCING DIAMETER

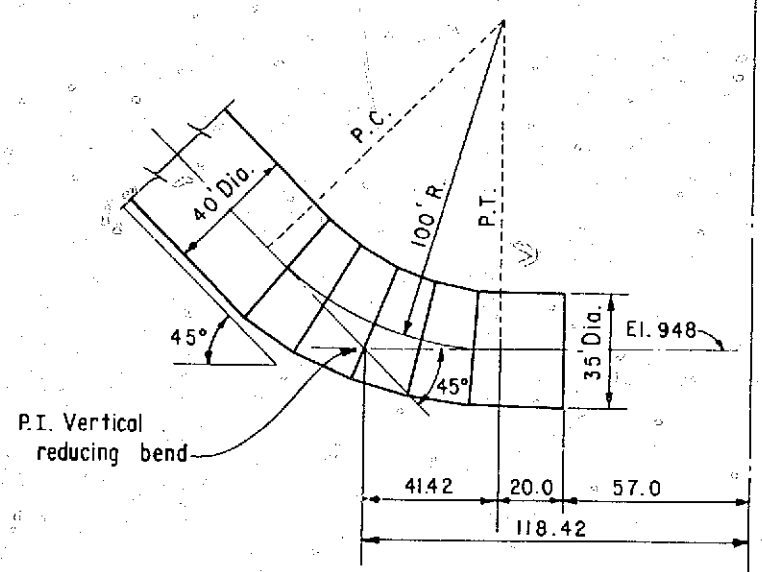

C. 100-FOOT RADIUS REDUCING DIAMETER (INSTALLED)

Figure 20. Lower elbow studies.

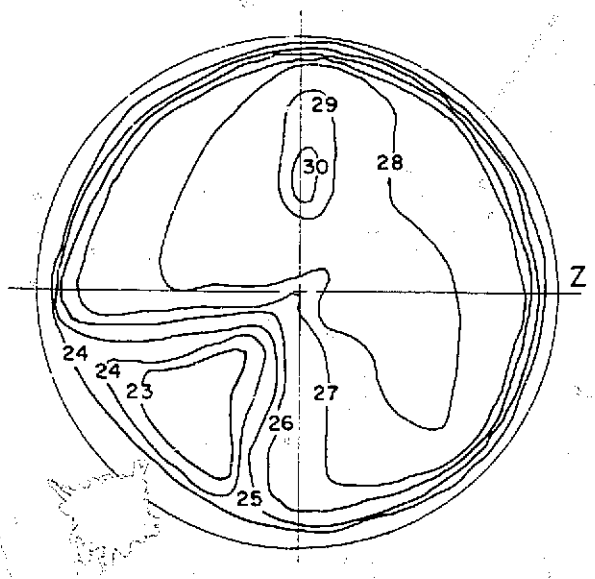

VELOCITY PATTERN IN
40-FT. DIAMETER PENSTOCK U.S.
FROM P.C. OF LOWER BEND

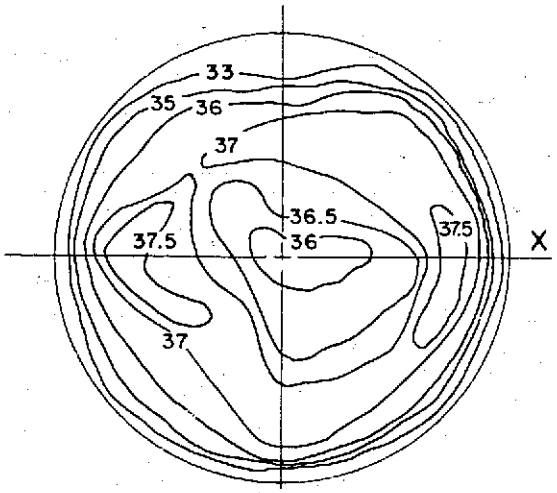

VELOCITY PATTERN IN
35-FT. DIAMETER PENSTOCK D.S.
FROM P.T. OF 100 FT. RADIUS
REDUCING DIAMETER BEND

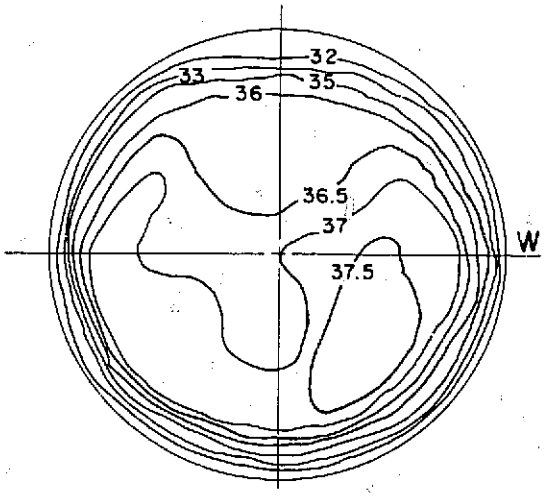

VELOCITY PATTERN IN
35-FT. DIAMETER PENSTOCK D.S.
FROM P.T. OF 140 FT. RADIUS
REDUCING BEND

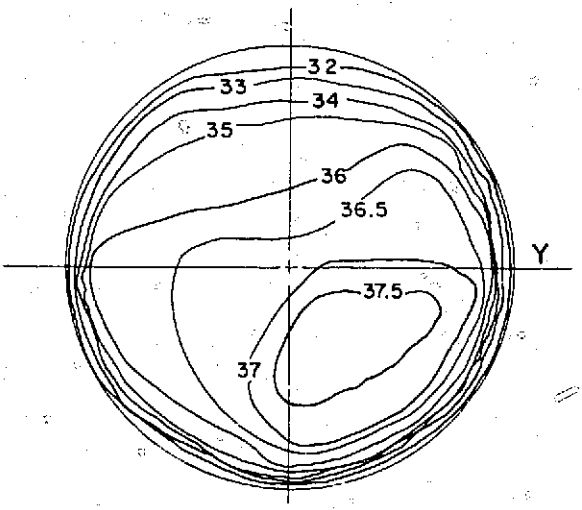

VELOCITY PATTERN IN
35-FT. DIAMETER PENSTOCK D.S.
FROM 100 FT. RADIUS BEND
WITH REDUCING CONE

Figure 21. Effect of bend configuration on velocity distribution.

For the first trial of a smaller entrance, an entrance area to penstock area ratio of 0.9:1 was selected. The 1-1/2:1 height-to-width ratio and the geometry of the entrance curves of the larger entrance were retained, Figure 22. The 40-foot (12.2-meter) long transition between the entrance section and the penstock was also retained, although the geometry of the transition was modified to accommodate the change in area.

Three tests made to evaluate this entrance were the head loss caused by the entrance and transition, the pressure distribution along the boundaries, and the degree of turbulence at the same piezometers used to measure the pressure distribution. As a result of these tests, velocity traverses in the penstock were not made.

Head loss.—The head loss measurements were taken for a model Reynolds number range from 3×10^5 to 1.1×10^6, the same as for the other entrances. The head loss coefficient for this entrance ranged from about 0.17 at the low Reynolds number to 0.12 for the high value, Figure 23. From the shape of the curve, the projected prototype head loss coefficient would probably be about 0.12 compared to 0.08 for the larger entrance.

Pressure distribution.—Piezometers to measure the pressure distribution were placed on the right and left side centerlines, the top right corner, and the top centerline.

The pressure drop coefficients obtained from these measurements showed excessively high pressure drop both at the entrance and through the rectangular-to-circular transition, Figure 24. Instantaneous pressure fluctuations at these piezometers were also greater than had been noted in the recommended design. At most piezometers the fluctuations were from 2 to 6 feet (0.06 to 0.18 meter) of water in magnitude at a frequency of about 2 hertz.

Because of the adverse flow conditions in this entrance, no further tests were made and it was considered inadvisable to investigate smaller entrances.

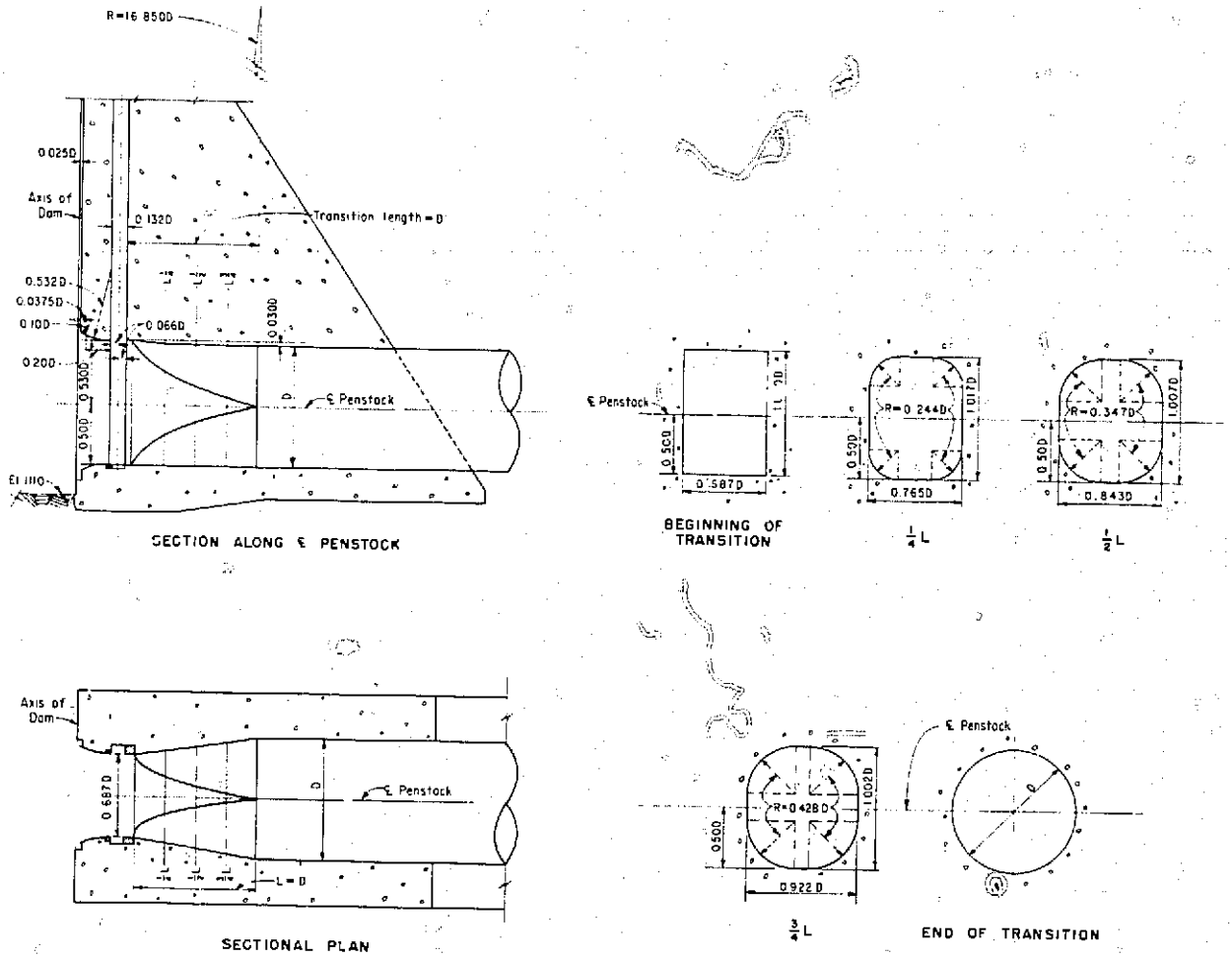

Figure 22. 0.9:1 ratio of entrance area to penstock area.

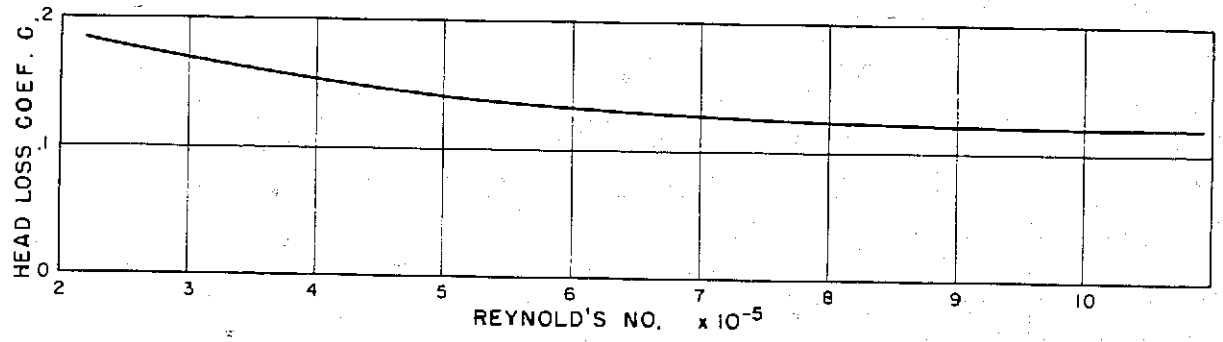

Head Loss $= C\frac{V^2}{2g}$ where V = Velocity in 40' Dia. Penstock
0.9:1 Ratio of Entrance Area to Penstock Area

Figure 23. Entrance head loss.

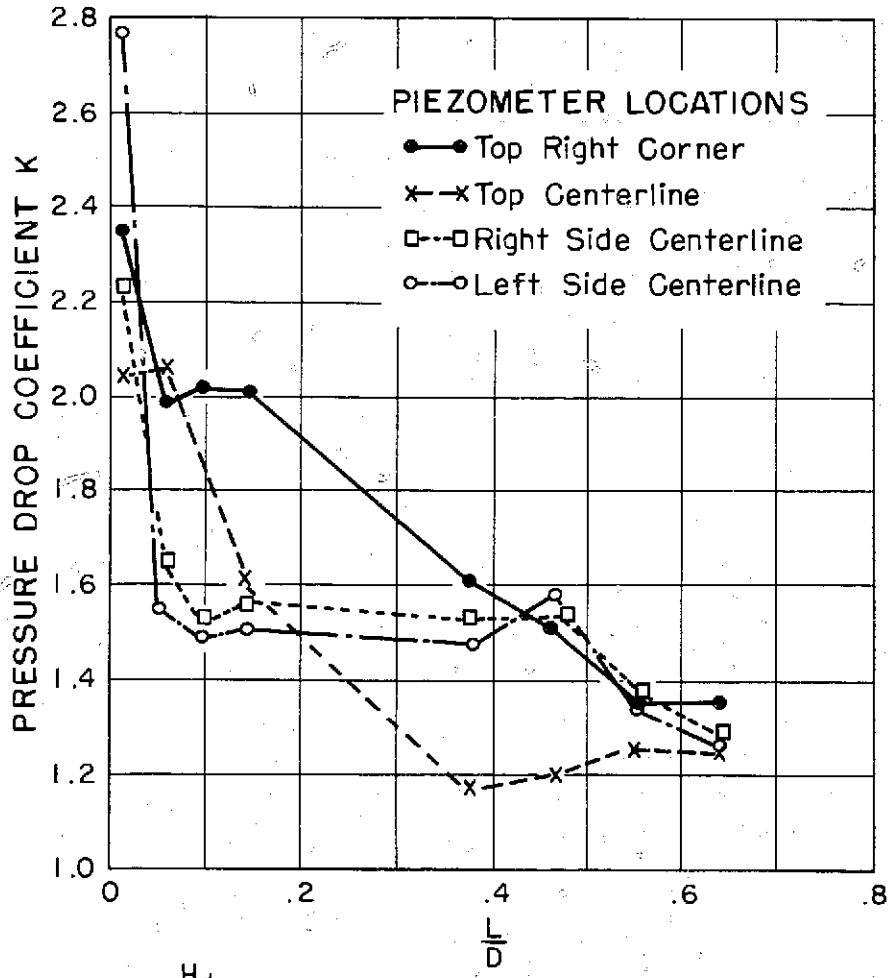

$K = \frac{H_d}{\frac{V^2}{2g}}$ where H_d = Pressure drop from reservoir to piezometer. V = Velocity in penstock.

L = Horizontal distance from face of entrance.

D = Penstock diameter.

PENSTOCK ENTRANCE

Figure 24. 0.9:1 ratio of entrance area to penstock area, pressure distribution.

APPENDIX

The oscillograms shown in this appendix are instantaneous pressures obtained from a pressure transducer on the impact line of a pitot cylinder. The dimensions shown are in model values and should be multiplied by the model scale, 41.74, to obtain prototype dimensions. The heavier lines of the horizontal time scale are 1-second intervals in the model, equivalent to approximately 6.5 prototype seconds. The space between the heavier horizontal grid lines (5 spaces between the lighter grid lines) on the vertical or magnitude scale is equivalent to 0.25 feet (7.5 cm) of water in the model, or about 10.5 feet (3.2 meters) of water prototype. All the measurements were made at a discharge equivalent to 35,000 cfs (990 cu m/sec). Plates 1 to 8 show the pressure fluctuations with the recommended entrance; Plates 9 to 16 show pressure fluctuations with the flared entrance.

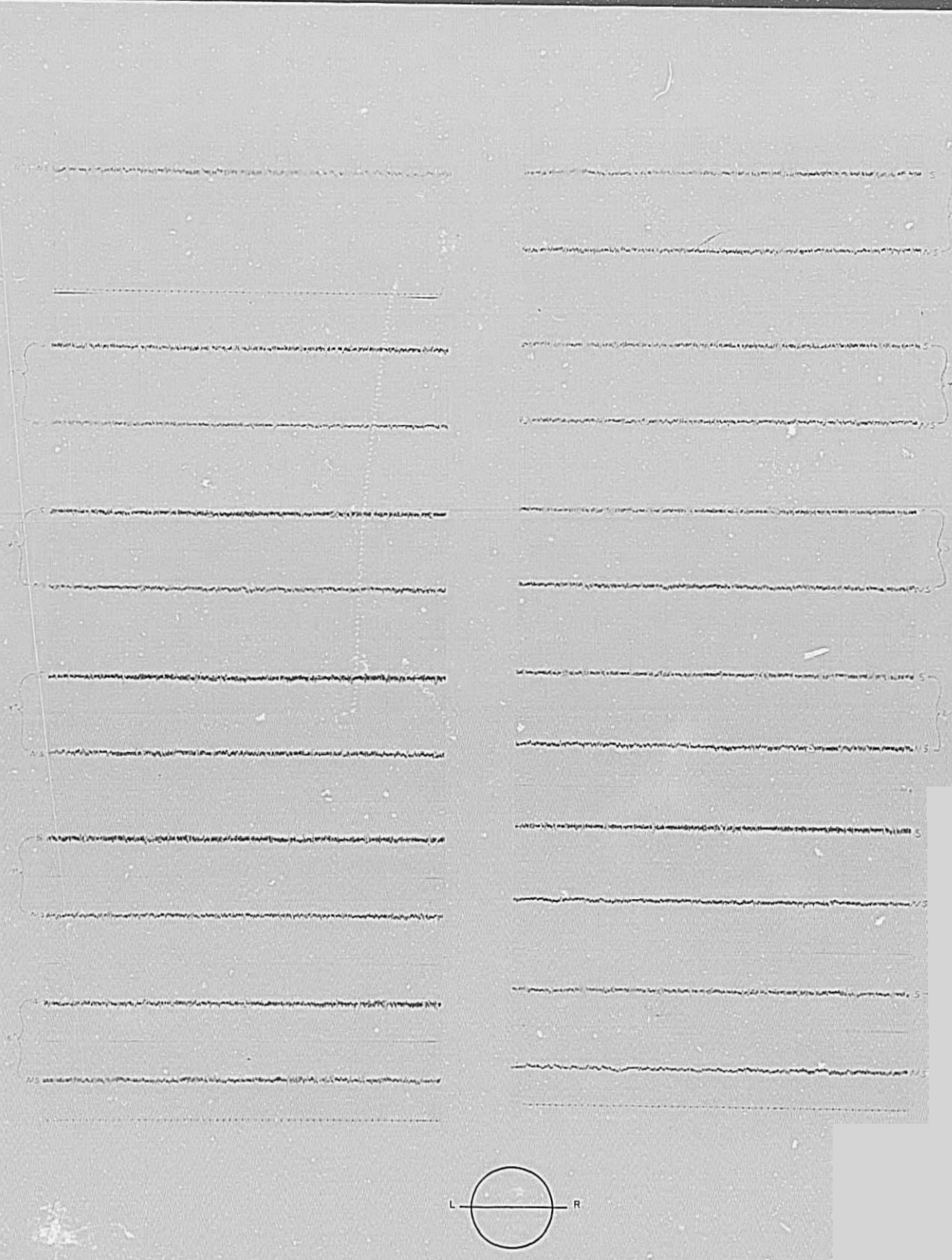

IMPACT HEADS FOR HORIZONTAL TRAVERSE–SYMMETRICAL (S) AND NONSYMMETRICAL (NS) READINGS IN STEPS FROM LEFT WALL
11-1/2" CONDUIT

PLATE 1

IMPACT HEADS
HORIZONTAL TRAVERSE
10" CONDUIT
DISTANCES ARE INCHES FROM LEFT SIDE

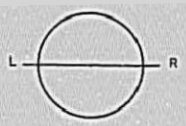

PLATE 2

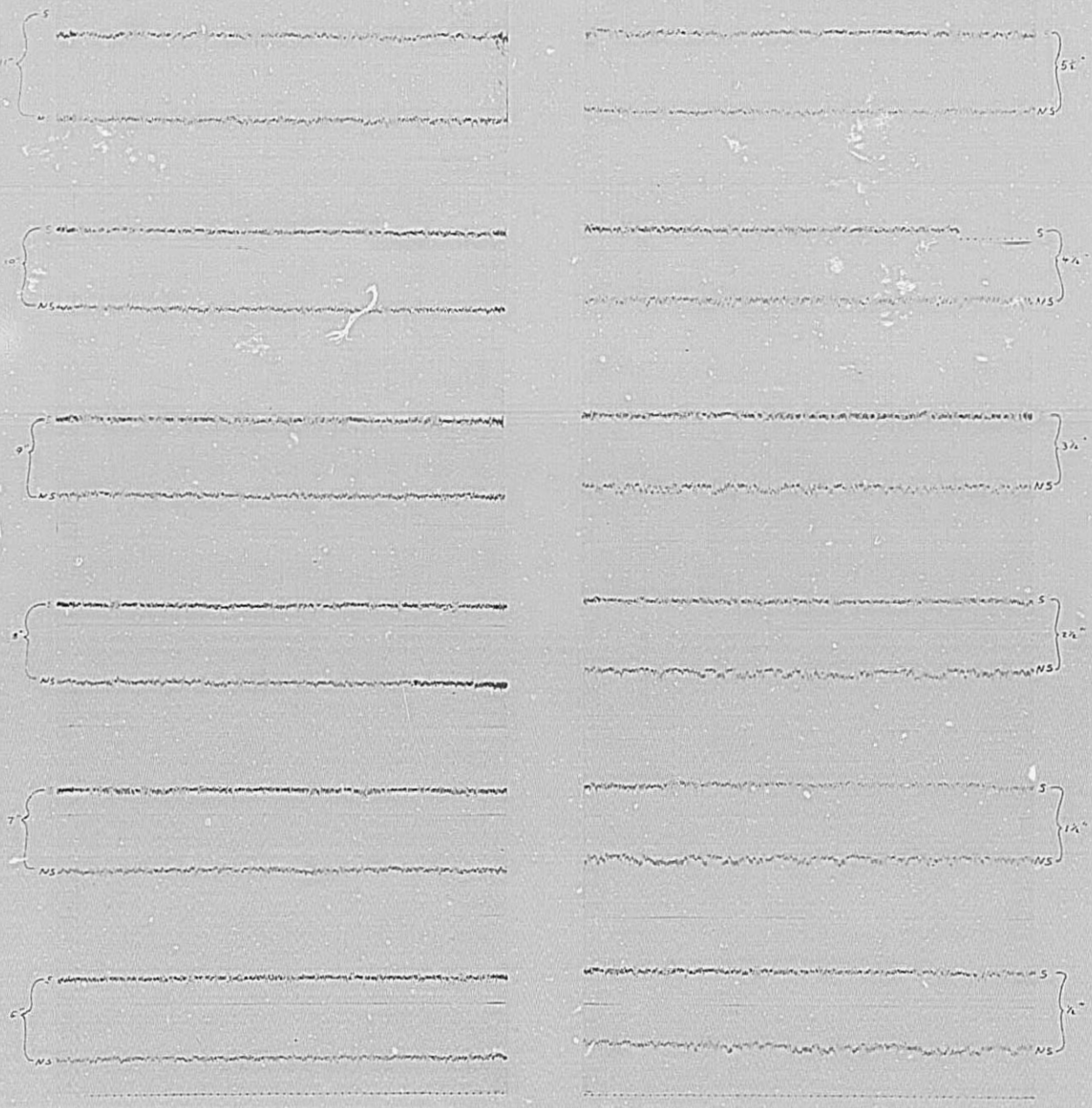

IMPACT HEADS FOR VERTICAL
TRAVERSE–11-1/2" CONDUIT
SYMMETRICAL (S) VS. NONSYMMETRICAL (NS)
READINGS IN STEPS FROM INVERT LINE

PLATE 3

IMPACT HEADS
VERTICAL TRAVERSE
10" CONDUIT
DISTANCES ARE INCHES ABOVE INVERT

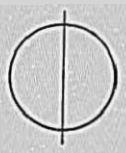

PLATE 4

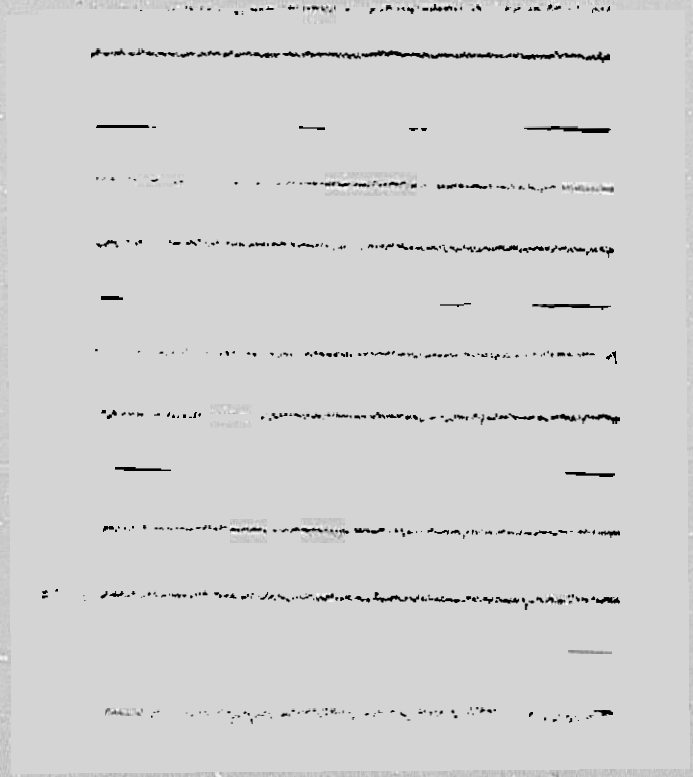

IMPACT HEADS
DIAGONAL FROM LEFT TRAVERSE
11-1/2" CONDUIT
DISTANCES ARE INCHES FROM LEFT SIDE

PLATE 5

IMPACT HEADS
DIAGONAL FROM LEFT TRAVERSE
10" CONDUIT
DISTANCES ARE INCHES FROM LEFT SIDE

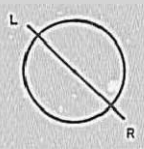

PLATE 6

IMPACT HEADS
DIAGONAL FROM RIGHT TRAVERSE
11-1/2" CONDUIT
DISTANCES ARE INCHES FROM LEFT SIDE

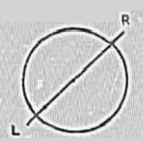

PLATE 7

IMPACT HEADS
DIAGONAL FROM RIGHT TRAVERSE
10" CONDUIT
DISTANCES ARE INCHES FROM LEFT SIDE

PLATE 8

FLARED ENTRANCE

IMPACT HEADS
HORIZONTAL TRAVERSE
11-1/2" CONDUIT
DISTANCES ARE INCHES FROM LEFT SIDE

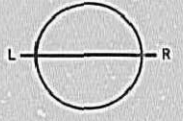

PLATE 9

FLARED ENTRANCE

IMPACT HEADS
VERTICAL TRAVERSE
11-1/2" CONDUIT
DISTANCES ARE INCHES ABOVE INVERT

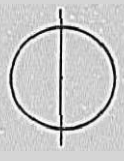

PLATE 10

FLARED ENTRANCE

IMPACT HEADS
VERTICAL TRAVERSE
10" CONDUIT
DISTANCES ARE INCHES ABOVE INVERT

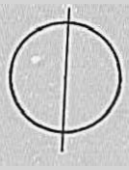

PLATE 11

FLARED ENTRANCE

IMPACT HEADS
HORIZONTAL TRAVERSE
10" CONDUIT
DISTANCES ARE INCHES FROM LEFT SIDE

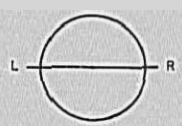

PLATE 12

FLARED ENTRANCE

IMPACT HEADS
DIAGONAL FROM RIGHT TRAVERSE
11-1/2" CONDUIT
DISTANCES ARE INCHES FROM LEFT SIDE

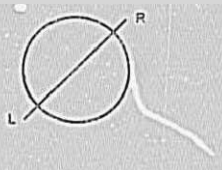

PLATE 13

IMPACT HEADS
DIAGONAL FROM RIGHT TRAVERSE
10" CONDUIT
DISTANCES ARE INCHES FROM LEFT SIDE

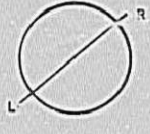

PLATE 14

FLARED ENTRANCE

IMPACT HEADS
DIAGONAL FROM LEFT TRAVERSE
11-1/2" CONDUIT
DISTANCES ARE INCHES FROM LEFT SIDE

PLATE 15

FLARED ENTRANCE

IMPACT HEADS
DIAGONAL FROM LEFT TRAVERSE
10" CONDUIT
DISTANCES ARE INCHES FROM LEFT SIDE

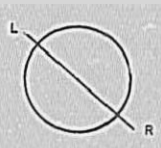

PLATE 16

7-1750 (3-71)
Bureau of Reclamation

CONVERSION FACTORS—BRITISH TO METRIC UNITS OF MEASUREMENT

The following conversion factors adopted by the Bureau of Reclamation are those published by the American Society for Testing and Materials (ASTM Metric Practice Guide, E 380-68) except that additional factors (*) commonly used in the Bureau have been added. Further discussion of definitions of quantities and units is given in the ASTM Metric Practice Guide.

The metric units and conversion factors adopted by the ASTM are based on the "International System of Units" (designated SI for Systeme International d'Unites), fixed by the International Committee for Weights and Measures; this system is also known as the Giorgi or MKSA (meter-kilogram (mass)-second-ampere) system. This system has been adopted by the International Organization for Standardization in ISO Recommendation R-31.

The metric technical unit of force is the kilogram-force; this is the force which, when applied to a body having a mass of 1 kg, gives it an acceleration of 9.80665 m/sec/sec, the standard acceleration of free fall toward the earth's center for sea level at 45 deg latitude. The metric unit of force in SI units is the newton (N), which is defined as that force which, when applied to a body having a mass of 1 kg, gives it an acceleration of 1 m/sec/sec. These units must be distinguished from the (inconstant) local weight of a body having a mass of 1 kg, that is, the weight of a body is that force with which a body is attracted to the earth and is equal to the mass of a body multiplied by the acceleration due to gravity. However, because it is general practice to use "pound" rather than the technically correct term "pound-force," the term "kilogram" (or derived mass unit) has been used in this guide instead of "kilogram-force" in expressing the conversion factors for forces. The newton unit of force will find increasing use, and is essential in SI units.

Where approximate or nominal English units are used to express a value or range of values, the converted metric units in parentheses are also approximate or nominal. Where precise English units are used, the converted metric units are expressed as equally significant values.

Table I

QUANTITIES AND UNITS OF SPACE

Multiply	By	To obtain
LENGTH		
Mil	25.4 (exactly)	Micron
Inches	25.4 (exactly)	Millimeters
Inches	2.54 (exactly)*	Centimeters
Feet	30.48 (exactly)	Centimeters
Feet	0.3048 (exactly)*	Meters
Feet	0.0003048 (exactly)*	Kilometers
Yards	0.9144 (exactly)	Meters
Miles (statute)	1,609.344 (exactly)*	Meters
Miles	1.609344 (exactly)	Kilometers
AREA		
Square inches	6.4516 (exactly)	Square centimeters
Square feet	*929.03	Square centimeters
Square feet	0.092903	Square meters
Square yards	0.836127	Square meters
Acres	***0.40469**	**Hectares**
Acres	*4,046.9	Square meters
Acres	*0.0040469	Square kilometers
Square miles	2.58999	Square kilometers
VOLUME		
Cubic inches	16.3871	Cubic centimeters
Cubic feet	0.0283168	Cubic meters
Cubic yards	0.764555	Cubic meters
CAPACITY		
Fluid ounces (U.S.)	29.5737	Cubic centimeters
Fluid ounces (U.S.)	29.5729	Milliliters
Liquid pints (U.S.)	0.473179	Cubic decimeters
Liquid pints (U.S.)	0.473166	Liters
Quarts (U.S.)	***946.358**	**Cubic centimeters**
Quarts (U.S.)	*0.946331	Liters
Gallons (U.S.)	*3,785.43	Cubic centimeters
Gallons (U.S.)	3.78543	Cubic decimeters
Gallons (U.S.)	3.78533	Liters
Gallons (U.S.)	***0.00378543**	**Cubic meters**
Gallons (U.K.)	4.54609	Cubic decimeters
Gallons (U.K.)	4.54596	Liters
Cubic feet	28.3160	Liters
Cubic yards	***764.55**	**Liters**
Acre-feet	*1,233.5	Cubic meters
Acre-feet	*1,233,500	Liters

Table II

QUANTITIES AND UNITS OF MECHANICS

Multiply	By	To obtain
MASS		
Grains (1/7,000 lb)	64.79891 (exactly)	Milligrams
Troy ounces (480 grains)	31.1035	Grams
Ounces (avdp)	28.3495	Grams
Pounds (avdp)	0.45359237 (exactly)	Kilograms
Short tons (2,000 lb)	907.185	Kilograms
Short tons (2,000 lb)	0.907185	Metric tons
Long tons (2,240 lb)	1,016.05	Kilograms
FORCE/AREA		
Pounds per square inch	0.070307	Kilograms per square centimeter
Pounds per square inch	0.689476	Newtons per square centimeter
Pounds per square foot	4.88243	Kilograms per square meter
Pounds per square foot	47.8803	Newtons per square meter
MASS/VOLUME (DENSITY)		
Ounces per cubic inch	1.72999	Grams per cubic centimeter
Pounds per cubic foot	16.0185	Kilograms per cubic meter
Pounds per cubic foot	0.0160185	Grams per cubic centimeter
Tons (long) per cubic yard	1.32894	Grams per cubic centimeter
MASS/CAPACITY		
Ounces per gallon (U.S.)	7.4893	Grams per liter
Ounces per gallon (U.K.)	6.2362	Grams per liter
Pounds per gallon (U.S.)	119.829	Grams per liter
Pounds per gallon (U.K.)	99.779	Grams per liter
BENDING MOMENT OR TORQUE		
Inch-pounds	0.011521	Meter-kilograms
Inch-pounds	1.12985×10^6	Centimeter-dynes
Foot-pounds	0.138255	Meter-kilograms
Foot-pounds	1.35582×10^7	Centimeter-dynes
Foot-pounds per inch	5.4431	Centimeter-kilograms per centimeter
Ounce-inches	72.008	Gram-centimeters
VELOCITY		
Feet per second	30.48 (exactly)	Centimeters per second
Feet per second	0.3048 (exactly)*	Meters per second
Feet per year	$*0.965873 \times 10^{-6}$	Centimeters per second
Miles per hour	1.609344 (exactly)	Kilometers per hour
Miles per hour	0.44704 (exactly)	Meters per second
ACCELERATION*		
Feet per second^2	*0.3048	Meters per second^2
FLOW		
Cubic feet per second (second-feet)	*0.028317	Cubic meters per second
Cubic feet per minute	0.4719	Liters per second
Gallons (U.S.) per minute	0.06309	Liters per second
FORCE*		
Pounds	*0.453592	Kilograms
Pounds	*4.4482	Newtons
Pounds	$*4.4482 \times 10^5$	Dynes

Table II—Continued

Multiply	By	To obtain
WORK AND ENERGY*		
British thermal units (Btu)	*0.252	Kilogram calories
British thermal units (Btu)	1,055.06	Joules
Btu per pound	2.326 (exactly)	Joules per gram
Foot-pounds	*1.35582	Joules
POWER		
Horsepower	745.700	Watts
Btu per hour	0.293071	Watts
Foot-pounds per second	1.35582	Watts
HEAT TRANSFER		
Btu in./hr ft^2 degree F (k, thermal conductivity)	1.442	Milliwatts/cm degree C
Btu in./hr ft^2 degree F (k, thermal conductivity)	0.1240	Kg cal/hr m degree C
Btu ft/hr ft^2 degree F	*1.4880	Kg cal m/hr m^2 degree C
Btu/hr ft^2 degree F (C, thermal conductance)	0.568	Milliwatts/cm^2 degree C
Btu/hr ft^2 degree F (C, thermal conductance)	4.882	Kg cal/hr m^2 degree C
Degree F hr ft^2/Btu (R, thermal resistance)	1.761	Degree C cm^2/milliwatt
Btu/lb degree F (c, heat capacity)	4.1868	J/g degree C
Btu/lb degree F	*1.000	Cal/gram degree C
Ft^2/hr (thermal diffusivity)	0.2581	Cm^2/sec
Ft^2/hr (thermal diffusivity)	*0.09290	M^2/hr
WATER VAPOR TRANSMISSION		
Grains/hr ft^2 (water vapor transmission)	16.7	Grams/24 hr m^2
Perms (permeance)	0.659	Metric perms
Perm-inches (permeability)	1.67	Metric perm-centimeters

Table III

OTHER QUANTITIES AND UNITS

Multiply	By	To obtain
Cubic feet per square foot per day (seepage)	*304.8	Liters per square meter per day
Pound-seconds per square foot (viscosity)	*4.8824	Kilogram second per square meter
Square feet per second (viscosity)	*0.092903	Square meters per second
Fahrenheit degrees (change)*	5/9 exactly	Celsius or Kelvin degrees (change)*
Volts per mil	0.03937	Kilovolts per millimeter
Lumens per square foot (foot-candles)	10.764	Lumens per square meter
Ohm-circular mils per foot	0.001662	Ohm-square millimeters per meter
Millicuries per cubic foot	*35.3147	Millicuries per cubic meter
Milliamps per square foot	*10.7639	Milliamps per square meter
Gallons per square yard	*4.527219	Liters per square meter
Pounds per inch	*0.17858	Kilograms per centimeter

GPO 835 - 186

ABSTRACT

Hydraulic model investigations were performed on a 1:41.75 scale model to aid in the design of the penstock entrances and lower bends of the Third Powerplant at Grand Coulee Dam. The initial entrance with a 2:1 height-to-width ratio, entrance area equal to penstock area, and a small radius entrance curve indicated excessive head loss and poor pressure distribution along the flow surfaces. A longer compound radius entrance curve reduced the head loss and improved the pressure distribution along the flow surfaces. A more economical entrance with a 1-1/2:1 height-to-width ratio and the compound radius entrance curve showed excellent hydraulic characteristics and was selected for prototype installation. The proposed trashrack will add to the head loss but will not affect other flow conditions. A model with flared entrance curves on the left side and roof was also tested but showed no significant improvements in flow characteristics. A model with the entrance area equal to 9/10 the penstock area indicated excessive head loss and poor pressure conditions. Vortex observations indicated the possibility of air-entraining vortices with all entrances tested. More detailed vortex studies on another model will be reported separately. Three types of lower bends were investigated. None showed any particular hydraulic advantage.

ABSTRACT

Hydraulic model investigations were performed on a 1:41.75 scale model to aid in the design of the penstock entrances and lower bends of the Third Powerplant at Grand Coulee Dam. The initial entrance with a 2:1 height-to-width ratio, entrance area equal to penstock area, and a small radius entrance curve indicated excessive head loss and poor pressure distribution along the flow surfaces. A longer compound radius entrance curve reduced the head loss and improved the pressure distribution along the flow surfaces. A more economical entrance with a 1-1/2:1 height-to-width ratio and the compound radius entrance curve showed excellent hydraulic characteristics and was selected for prototype installation. The proposed trashrack will add to the head loss but will not affect other flow conditions. A model with flared entrance curves on the left side and roof was also tested but showed no significant improvements in flow characteristics. A model with the entrance area equal to 9/10 the penstock area indicated excessive head loss and poor pressure conditions. Vortex observations indicated the possibility of air-entraining vortices with all entrances tested. More detailed vortex studies on another model will be reported separately. Three types of lower bends were investigated. None showed any particular hydraulic advantage.

ABSTRACT

Hydraulic model investigations were performed on a 1:41.75 scale model to aid in the design of the penstock entrances and lower bends of the Third Powerplant at Grand Coulee Dam. The initial entrance with a 2:1 height-to-width ratio, entrance area equal to penstock area, and a small radius entrance curve indicated excessive head loss and poor pressure distribution along the flow surfaces. A longer compound radius entrance curve reduced the head loss and improved the pressure distribution along the flow surfaces. A more economical entrance with a 1-1/2:1 height-to-width ratio and the compound radius entrance curve showed excellent hydraulic characteristics and was selected for prototype installation. The proposed trashrack will add to the head loss but will not affect other flow conditions. A model with flared entrance curves on the left side and roof was also tested but showed no significant improvements in flow characteristics. A model with the entrance area equal to 9/10 the penstock area indicated excessive head loss and poor pressure conditions. Vortex observations indicated the possibility of air-entraining vortices with all entrances tested. More detailed vortex studies on another model will be reported separately. Three types of lower bends were investigated. None showed any particular hydraulic advantage.

ABSTRACT

Hydraulic model investigations were performed on a 1:41.75 scale model to aid in the design of the penstock entrances and lower bends of the Third Powerplant at Grand Coulee Dam. The initial entrance with a 2:1 height-to-width ratio, entrance area equal to penstock area, and a small radius entrance curve indicated excessive head loss and poor pressure distribution along the flow surfaces. A longer compound radius entrance curve reduced the head loss and improved the pressure distribution along the flow surfaces. A more economical entrance with a 1-1/2:1 height-to-width ratio and the compound radius entrance curve showed excellent hydraulic characteristics and was selected for prototype installation. The proposed trashrack will add to the head loss but will not affect other flow conditions. A model with flared entrance curves on the left side and roof was also tested but showed no significant improvements in flow characteristics. A model with the entrance area equal to 9/10 the penstock area indicated excessive head loss and poor pressure conditions. Vortex observations indicated the possibility of air-entraining vortices with all entrances tested. More detailed vortex studies on another model will be reported separately. Three types of lower bends were investigated. None showed any particular hydraulic advantage.

REC-ERC-74-12
Rhone, T J
HYDRAULIC MODEL STUDIES FOR THE PENSTOCKS FOR GRAND COULEE THIRD POWERPLANT
Bur Reclam Rep REC-ERC-74-12, Div Gen Res, Aug 1974. Bureau of Reclamation, Denver, 41 p, 24 fig, 16 plate, append

DESCRIPTORS—/ bellmouths/ bends (hydraulic)/ *entrances (fluid flow)/ *head losses/ *hydraulic models/ intake structures/ *penstocks/ intake transitions/ trashracks/ turbulence/ *velocity distribution/ vortices/ prototypes/ model tests/ pressure distribution/ flow characteristics/ entrapped air
IDENTIFIERS—/ Grand Coulee Powerplant, WA

REC-ERC-74-12
Rhone, T J
HYDRAULIC MODEL STUDIES FOR THE PENSTOCKS FOR GRAND COULEE THIRD POWERPLANT
Bur Reclam Rep REC-ERC-74-12, Div Gen Res, Aug 1974. Bureau of Reclamation, Denver, 41 p, 24 fig, 16 plate, append

DESCRIPTORS—/ bellmouths/ bends (hydraulic)/ *entrances (fluid flow)/ *head losses/ *hydraulic models/ intake structures/ *penstocks/ intake transitions/ trashracks/ turbulence/ *velocity distribution/ vortices/ prototypes/ model tests/ pressure distribution/ flow characteristics/ entrapped air
IDENTIFIERS—/ Grand Coulee Powerplant, WA

REC-ERC-74-12
Rhone, T J
HYDRAULIC MODEL STUDIES FOR THE PENSTOCKS FOR GRAND COULEE THIRD POWERPLANT
Bur Reclam Rep REC-ERC-74-12, Div Gen Res, Aug 1974. Bureau of Reclamation, Denver, 41 p, 24 fig, 16 plate, append

DESCRIPTORS—/ bellmouths/ bends (hydraulic)/ *entrances (fluid flow)/ *head losses/ *hydraulic models/ intake structures/ *penstocks/ intake transitions/ trashracks/ turbulence/ *velocity distribution/ vortices/ prototypes/ model tests/ pressure distribution/ flow characteristics/ entrapped air
IDENTIFIERS—/ Grand Coulee Powerplant, WA

REC-ERC-74-12
Rhone, T J
HYDRAULIC MODEL STUDIES FOR THE PENSTOCKS FOR GRAND COULEE THIRD POWERPLANT
Bur Reclam Rep REC-ERC-74-12, Div Gen Res, Aug 1974. Bureau of Reclamation, Denver, 41 p, 24 fig, 16 plate, append

DESCRIPTORS—/ bellmouths/ bends (hydraulic)/ *entrances (fluid flow)/ *head losses/ *hydraulic models/ intake structures/ *penstocks/ intake transitions/ trashracks/ turbulence/ *velocity distribution/ vortices/ prototypes/ model tests/ pressure distribution/ flow characteristics/ entrapped air
IDENTIFIERS—/ Grand Coulee Powerplant, WA